united nations
educational, scientific
and cultural
organization

international atomic
energy agency

the
abdus salam
international centre for theoretical physics

ICTP 40th Anniversary

SMR.1555 - 26

Workshop on
Nuclear Reaction Data and Nuclear Reactors:
Physics, Design and Safety

16 February - 12 March 2004

Optical Model

Brett V. CARLSON
Centro Tecnico Aerospacial
Instituto Tecnologico de Aeronautica
Depto. de Fisica
Pr. Marechal Eduardo Gomes 50
Vila da Acacias
12228-900 Sao Jose dos Campos
BRAZIL

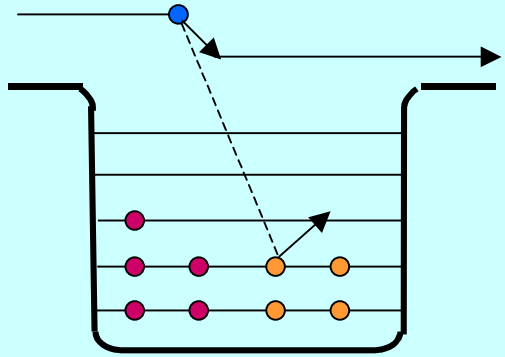

The Optical Model

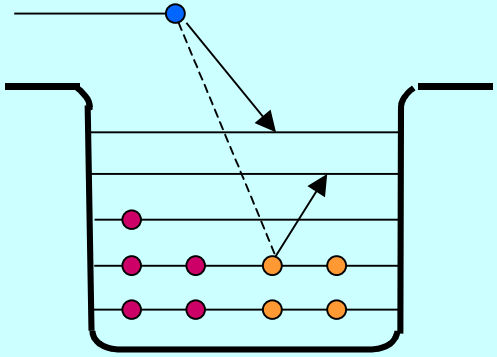

B.V. Carlson -- Depto. de Física
Instituto Tecnológico de Aeronáutica
São José dos Campos SP, Brazil

Nuclear scattering and reactions

- Elastic scattering – (n, n), (p, p), (α ,α), ...
- Inelastic Scattering -- (n, n′), (p, p′), (α ,α′), ...
- Knockout/emission – (n, 2n), (n, np), (p, pn), (p, 2p), ...
- Stripping – (d, p), (d, n), (t, d), ...
- Pickup – (p, d), (n, d), (d, t), ...
- Charge exchange – (n,p), (p,n), (t,^{3}He), (^{3}He, t), ...

The optical model is particularly important for the study of the direct (fast) contribution to nuclear reactions.

However, it also plays an important role in the analysis of the statistical (slow) contribution to nuclear reactions.

The Classical Cross Section

b – the impact parameter

- perpendicular distance between particle trajectory and center of target

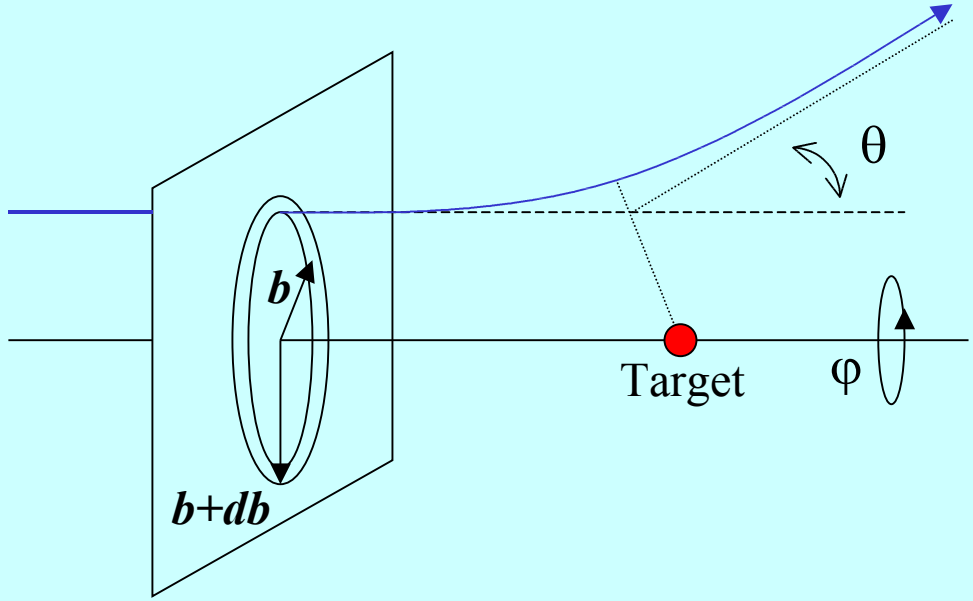

Assuming no dependence on φ,

$$\frac{d\sigma}{d\theta} = 2\pi\, b(\theta)\left|\frac{db}{d\theta}\right|$$

Since

$$d\Omega = 2\pi \sin\theta\, d\theta$$

$$\Rightarrow \quad \frac{d\sigma}{d\Omega} = \frac{b(\theta)}{\sin\theta}\left|\frac{db}{d\theta}\right|$$

An example – Hard sphere scattering

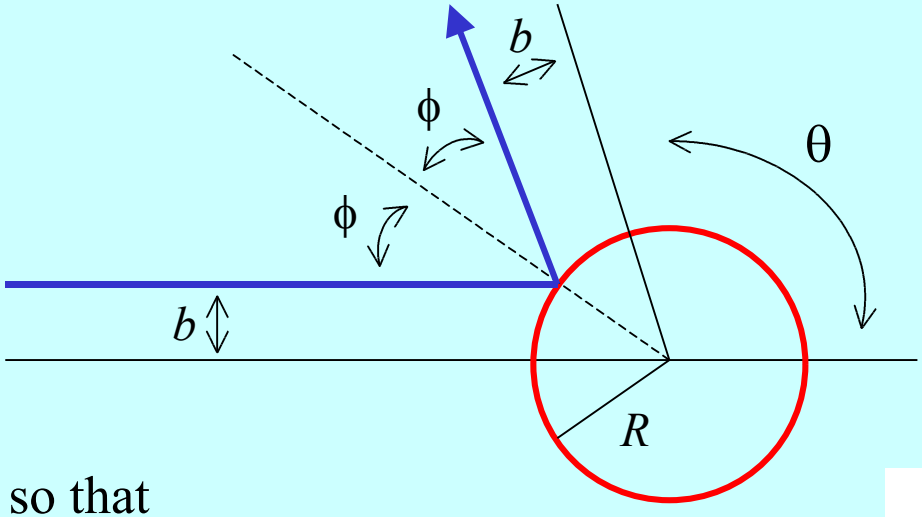

We have

$$b(\phi) = R\sin\phi$$

and

$$\phi = \frac{\pi - \theta}{2}.$$

so that

$$\frac{d\sigma}{d\theta} = 2\pi\, b(\theta)\left|\frac{db}{d\theta}\right| = \frac{\pi R^2}{2}\sin\theta$$

and

$$\frac{d\sigma}{d\Omega} = \frac{b(\theta)}{\sin\theta}\left|\frac{db}{d\theta}\right| = \frac{R^2}{4}$$

For ^{238}U, R ≈ 7.5 fm and

$R^2/4 \approx 14$ fm^2 = 140 mb.

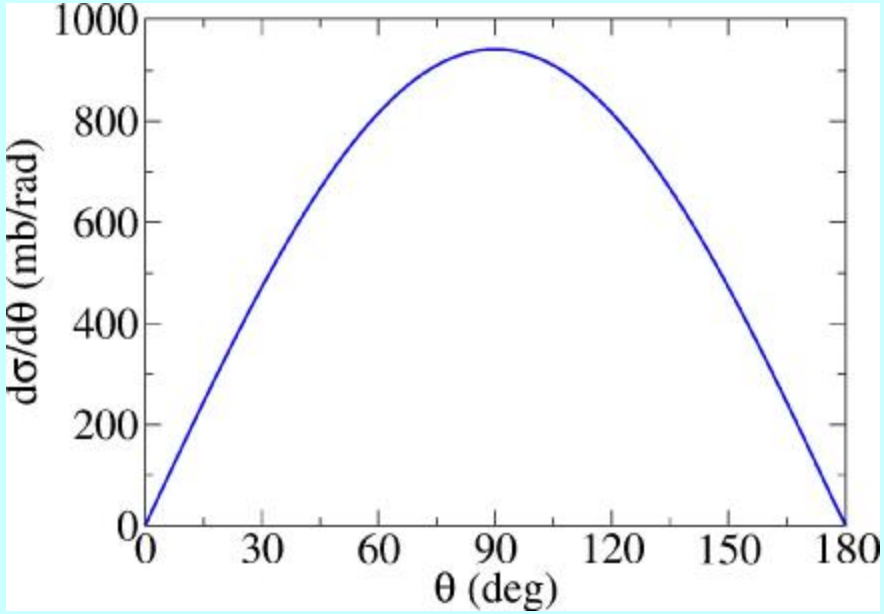

Another example – a sticky hard sphere

Now, suppose that a fraction of the incoming particles do not scatter, but instead stick to the target. Let us assume, for instance, that the fraction

$$P(\theta) = \alpha \cos\phi = \alpha \sin\frac{\theta}{2}$$

(which decreases as the collision becomes more grazing) is absorbed by the target.

Decomposition of the differential cross section:

$$\frac{d\sigma_{abs}}{d\theta} = \frac{\pi R^2}{2} P(\theta)\sin\theta$$

$$\frac{d\sigma_{el}}{d\theta} = \frac{\pi R^2}{2}\left(1 - P(\theta)\right)\sin\theta$$

$$\frac{d\sigma_{tot}}{d\theta} = \frac{d\sigma_{abs}}{d\theta} + \frac{d\sigma_{el}}{d\theta} = \frac{\pi R^2}{2}\sin\theta$$

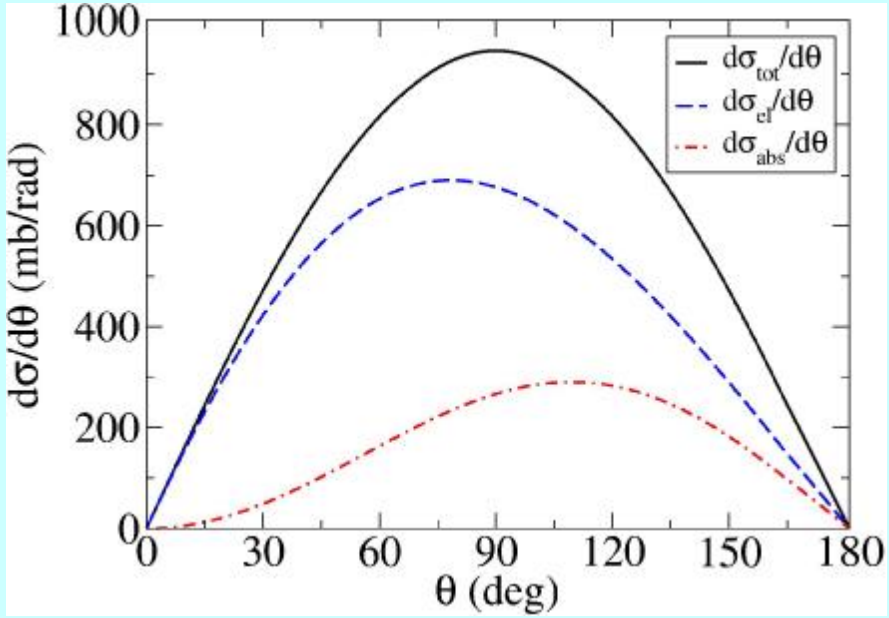

Only $d\sigma_{el}/d\theta$ is observed as scattered particles. In the figure, $\alpha = 0.4$

Integrated cross sections

We can integrate the differential cross sections over angle to obtain

$$\sigma_{abs} = \frac{\pi R^2}{2}\int_0^{\pi} P(\theta)\sin\theta\, d\theta = \frac{2}{3}\alpha\pi R^2$$

$$\sigma_{el} = \frac{\pi R^2}{2}\int_0^{\pi} \left(1-P(\theta)\right)\sin\theta\, d\theta = \left(1-\frac{2}{3}\alpha\right)\pi R^2$$

$$\sigma_{tot} = \sigma_{abs} + \sigma_{el} = \pi R^2$$

The total cross section of πR^2 is what we would expect and what we would obtain in the simple hard sphere case.

In the general case, when there is a value of the impact parameter b_{max} such that $\theta(b)=0$ for $b>b_{max}$, we have

$$\sigma_{tot} = 2\pi\int_0^{\pi} b(\theta)\left|\frac{db}{d\theta}\right| d\theta = \pi b^2\Big|_0^{b_{\max}} = \pi b_{\max}^2$$

Attenuation and the total cross section

Both elastic scattering and absorption remove particles from the incident beam. The sum of the two – the total cross section – determines how the beam is attenuated as it passes through the target.

From the definition of the cross section, we have in any dz

$$\sigma_{tot} = \frac{-dn}{n(z)\,\rho_{tar}\,dz}$$

or

$$\frac{dn}{dz} = -\rho_{tar}\,\sigma_{tot}\,n(z)$$

$$\Rightarrow \quad n(z) = n_0 \exp\left(-\rho_{tar}\,\sigma_{tot}\,z\right)$$

The inverse of the product $\rho_{tar}\sigma_{tot}$ defines the mean free path λ of the projectile through the target.

$$\lambda = 1/\rho_{tar}\sigma_{tot}$$

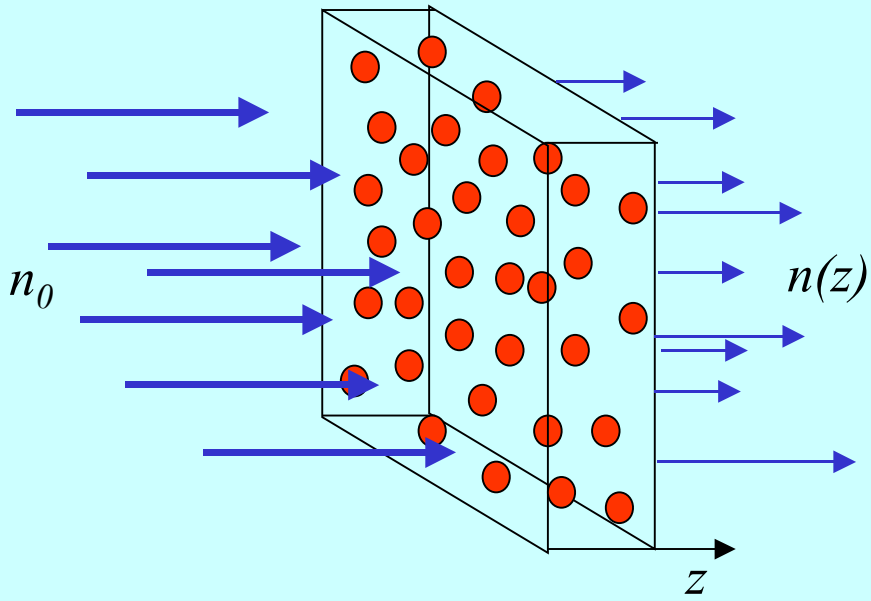

For our example of hard scattering from U-like spheres, assuming a density close to that of U, we have

$$\lambda = \left(\frac{19*6}{238}\times 10^{29} * 177 \times 10^{-30}\ \mathrm{m}^{-1}\right)^{-1} \approx 0.12\,\mathrm{m}$$

Yet another example – Coulomb scattering

Conservation of energy:

$$\frac{p_r^2}{2\mu}+\frac{p_{cm}^2}{2\mu}\frac{b^2}{r^2}+\frac{Z_P Z_T e^2}{r}=E_{cm}$$

with p_r the radial momentum and r the radial coordinate and $E_{cm}=p_{cm}^2/2\mu$.

When $b = 0$, the point of closest approach a_0 is given by

$$\frac{Z_P Z_T e^2}{a_0}=E_{cm} \quad \Rightarrow \quad a_0=\frac{Z_P Z_T e^2}{E_{cm}}$$

For arbitary b, the point of closest approach a satisfies

$$\frac{p_{cm}^2}{2\mu}\frac{b^2}{a^2}+\frac{Z_P Z_T e^2}{a}=E_{cm}$$

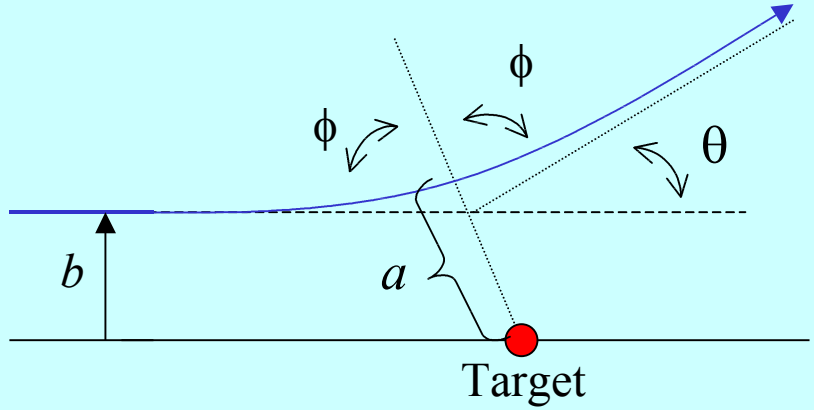

This becomes

$$b^2=a(a-a_0)$$

The orbit for repulsive Coulomb scattering forms a hyperbola satisfying

$$b=a\tan\left(\frac{\phi}{2}\right)$$

Substituting in the expression above, we obtain

$$b=\frac{a_0}{2}\tan\phi$$

Coulomb scattering – the differential cross section

Combining

$$\theta = \pi - 2\phi \quad \text{and} \quad b = \frac{a_0}{2}\tan\phi$$

we have

$$b = \frac{a_0}{2}\cot\left(\frac{\theta}{2}\right).$$

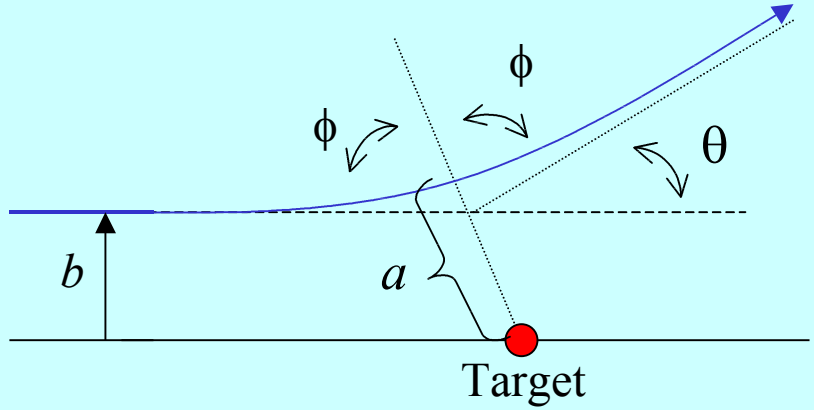

The differential cross section is then

$$\frac{d\sigma}{d\theta} = \pi\left(\frac{a_0}{2}\right)^2 \frac{\cos\left(\frac{\theta}{2}\right)}{\sin^3\left(\frac{\theta}{2}\right)}$$

or

$$\frac{d\sigma}{d\Omega} = \left(\frac{a_0}{4}\right)^2 \frac{1}{\sin^4\left(\frac{\theta}{2}\right)}.$$

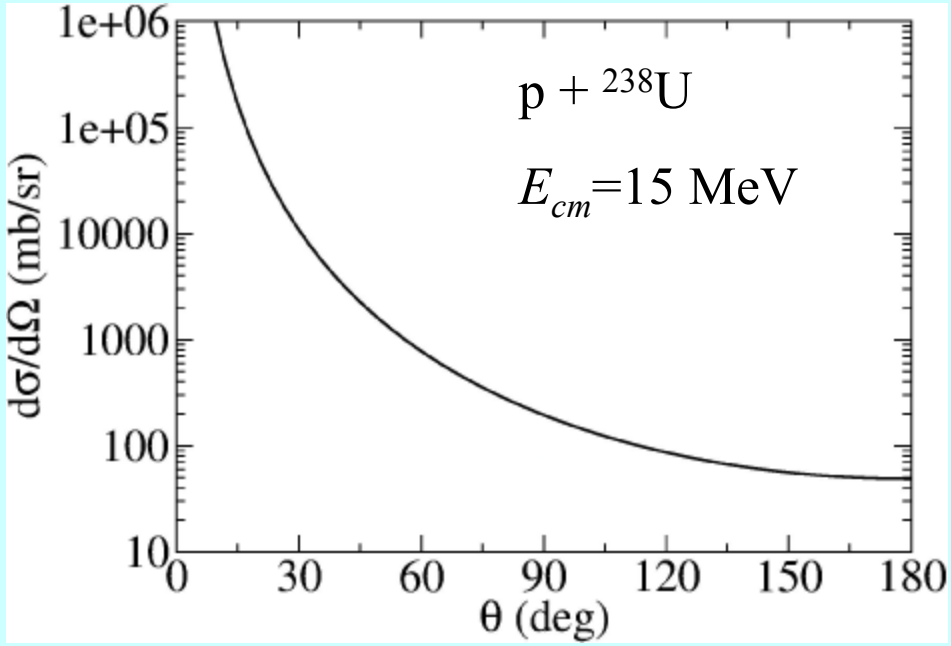

No integrated Coulomb cross section

It is obvious from its explicit form,

$$\frac{d\sigma}{d\Omega} = \left(\frac{a_0}{4}\right)^2 \frac{1}{\sin^4\left(\frac{\theta}{2}\right)}.$$

as well as from the figure, that the Coulomb angular distribution diverges at small angles.

This expression may be integrated formally,

$$\sigma = 2\pi \int_0^{\pi} \frac{d\sigma}{d\Omega} \sin\theta d\theta$$

$$= \pi \left(\frac{a_0}{2\sin(\theta/2)}\right)^2 \Bigg|_{\pi}^{0}$$

but is also divergent.

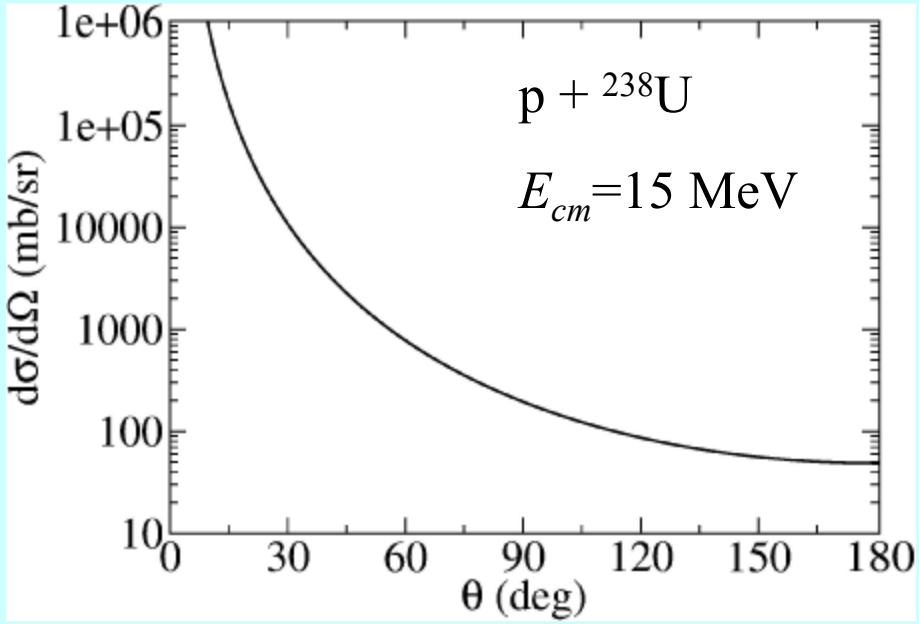

The long range of the Coulomb potential is the physical reason for the divergences in the Coulomb angular distribution and cross section. There is no value of the impact parameter b_{max} for which scattering no longer occurs.

Coulomb scattering from a charge distribution

In scattering calculations, the nuclear charge distribution is usually taken as that of a uniformly charged sphere of radius R_c=1.25*A$^{1/3}$ (fm).

$$V_C(r) = \begin{cases} \dfrac{Z_P Z_T e^2}{2R_C}\left(3-(r/R_C)^2\right) & r < R_C \\ \dfrac{Z_P Z_T e^2}{r} & r > R_C \end{cases}$$

Since the nuclear potential is short-ranged, the scattering at large values of the impact parameter is Coulomb scattering.

In the example given here, the scattering at angles below about 95° would be pure point-like Coulomb scattering.

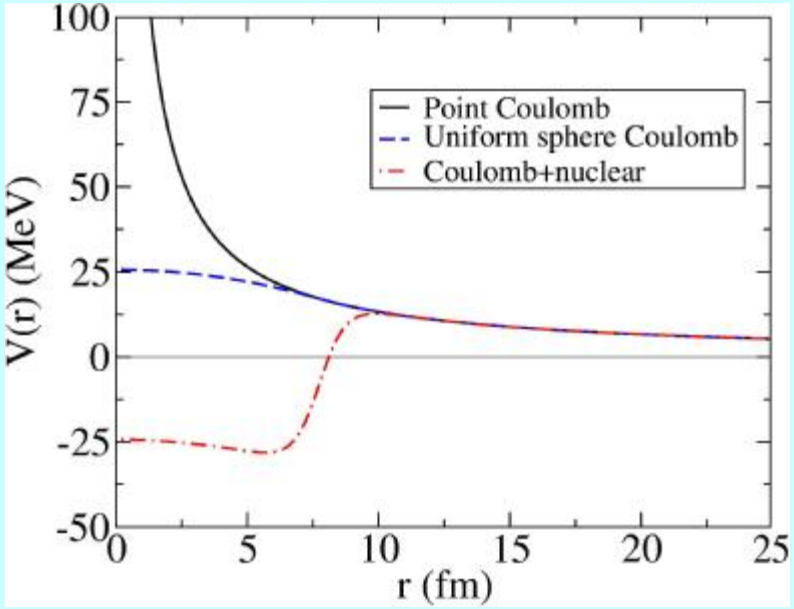

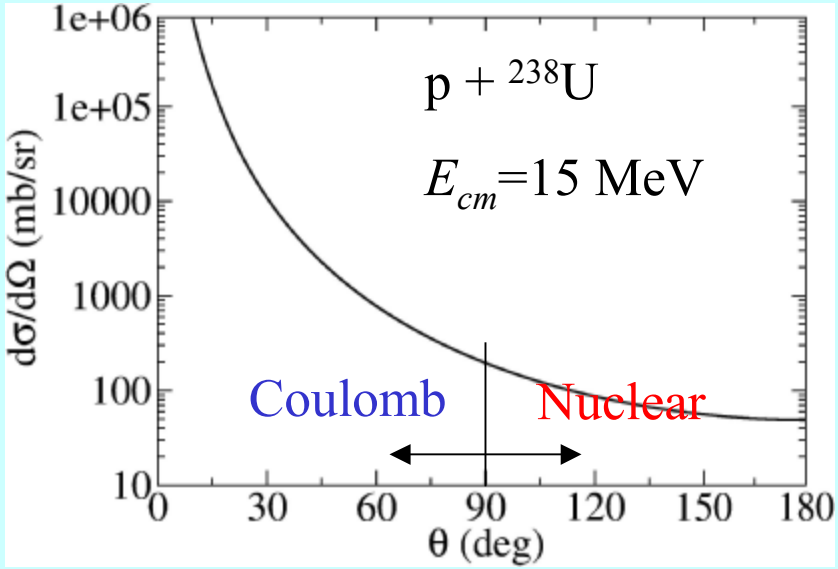

The Coulomb barrier for charged particles

The Coulomb + nuclear potential forms a barrier to charged particles that reaches its maximum just outside the nucleus. Outside the barrier maximum, the potential is very similar to the Coulomb potential of pointlike particles. At relative energies below the Coulomb barrier or at distances of closest approach greater than the barrier position, the scattering is almost purely point-like Coulomb scattering.

We can estimate the barrier position as

$$R_B \approx 1.25A^{1/3} + 2.0 \text{ (fm)}$$

and its height as

$$V_B \approx \frac{Z_P Z_T e^2}{R_B} \quad \text{(MeV)}.$$

The barrier height V_B for protons is shown at the right.

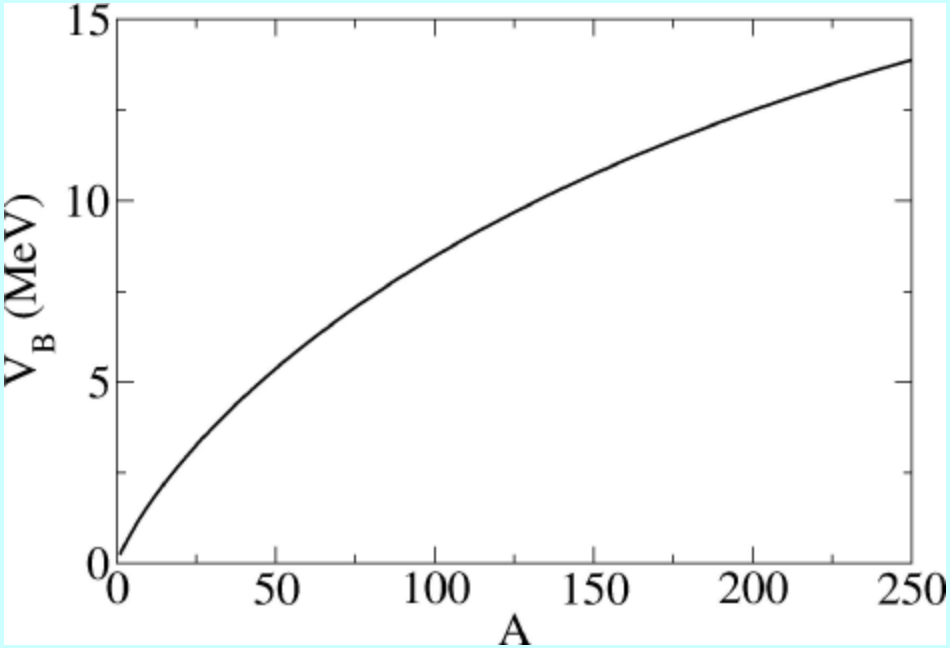

Waves and particles

We know that the wave-like nature of the scattering particles may be neglected only if their wavelength is much smaller than the length scale on which the scattering system varies. For nuclear scattering, the appropriate length scale would be at most the size of the nucleus and should probably be of the size of the nuclear surface – about 0.5 to 1.0 fm.

Comparing the wavelength of a nucleon to a typical nuclear radius, taken to be $R = 1.25A^{1/3}$ (fm), we find that the wavelike nature must be taken into account over the entire energy range we will consider – up to about 20 MeV.

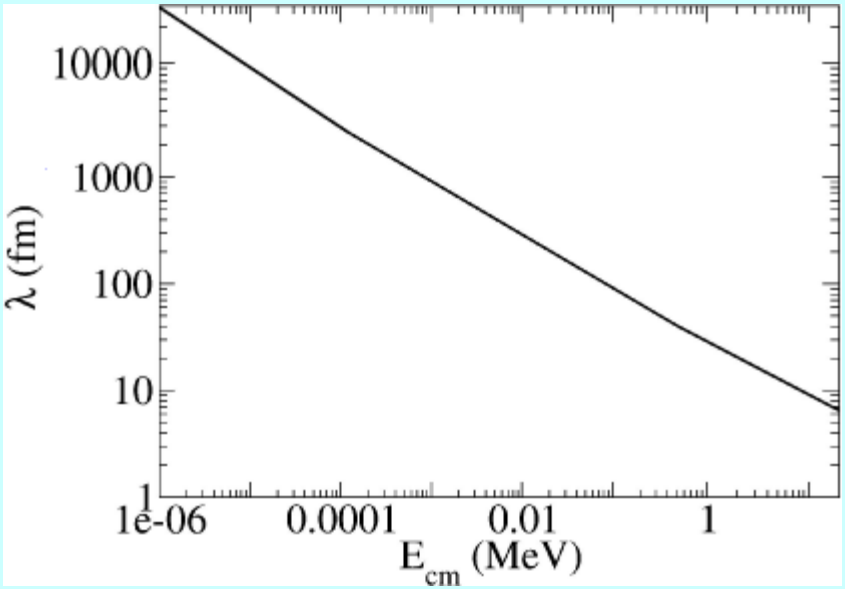

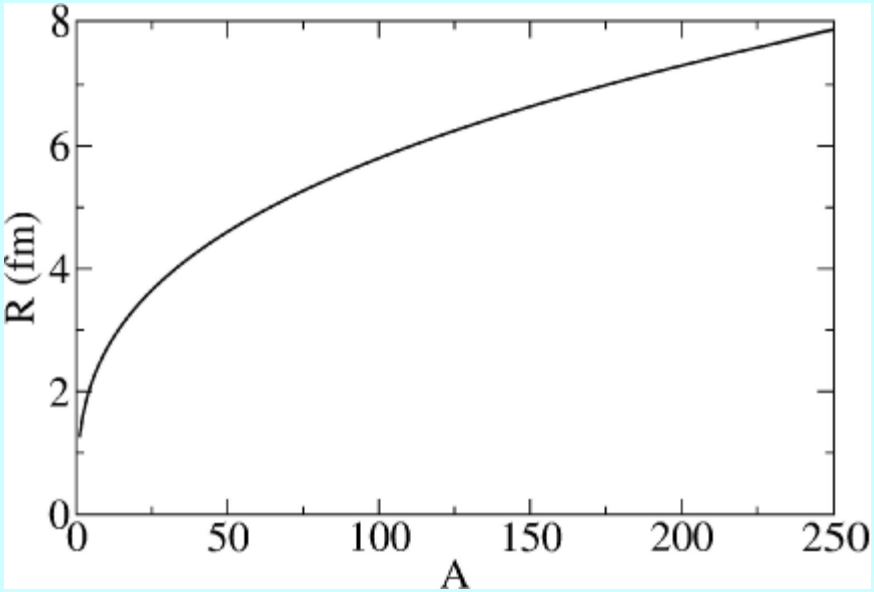

The quantum view of scattering

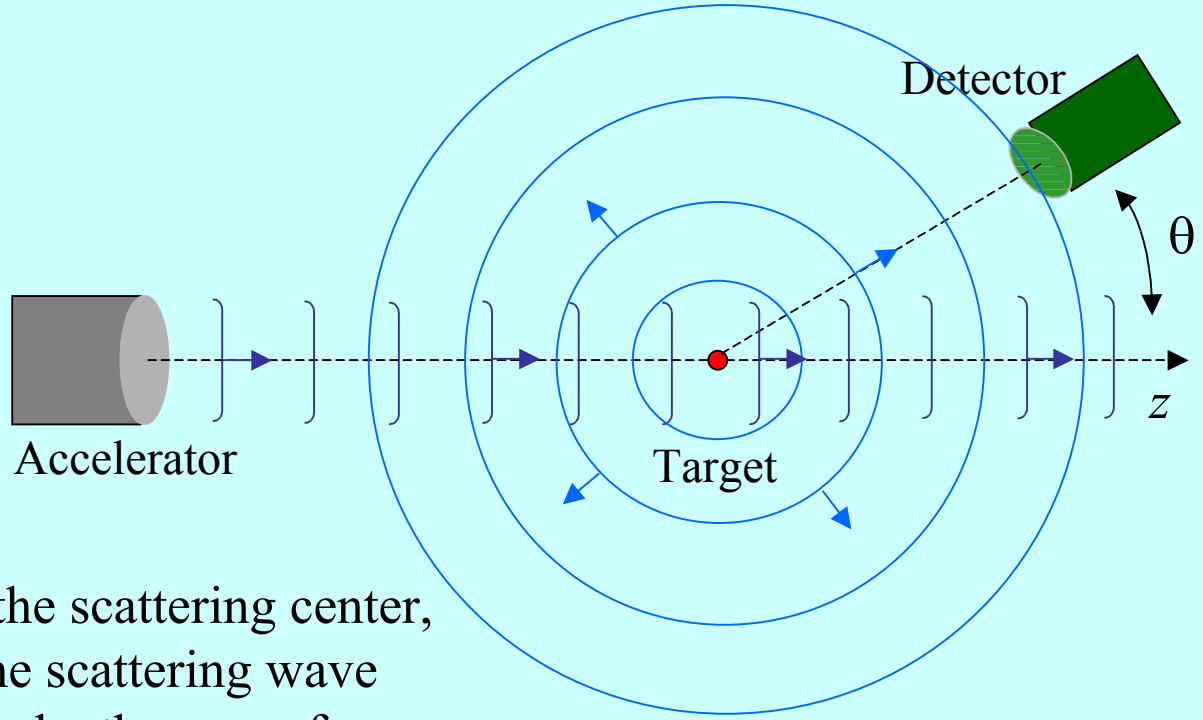

Far from the scattering center, we take the scattering wave function to be the sum of a plane wave and a scattered outgoing spherical wave,

$$\psi(\vec{r}) \approx e^{ikz} + f(\theta)\frac{e^{ikr}}{r}.$$

when $r \to \infty$. $\left(k^2 = 2\mu E_{cm}/\hbar^2\right)$

The differential cross section is the squared magnitude of the scattering amplitude,

$$\frac{d\sigma}{d\Omega} = \left|f(\theta)\right|^2.$$

Back to the basics

We defined the differential cross section as

$$d\sigma = \frac{\text{particle intensity entering detector of solid angle } d\Omega}{\text{(incident intensity/area) * (no. of target particles in beam)}} = \frac{n(\theta)\,d\Omega}{\left(n_0 / A\right)\left(\rho_{tar} tA\right)}$$

How did we relate this with the asymptotic form of the wave function

$$\psi(\vec{r}) \approx e^{ikz} + f(\theta)\frac{e^{ikr}}{r}. \qquad \text{to obtain} \qquad \frac{d\sigma}{d\Omega} = \left|f(\theta)\right|^2 ?$$

- First, we assume that we have but one target nucleus, $\rho_{tar} tA = 1$.
- Next, we note that n_0/A is proportional to the plane wave current density,

$$n_0 / A = \frac{\hbar}{2i\mu}\left(\psi_{in}^* \nabla \psi_{in} - \left(\nabla \psi_{in}^*\right)\psi_{in}\right) = \frac{\hbar k}{\mu} = v \quad \text{since} \quad \psi_{in} = e^{ikz}.$$

- Finally, we write the particle intensity entering the detector in terms of the current density of scattered particles,

$$n(r,\theta)d\Omega = \frac{\hbar}{2i\mu}\left(\psi_{sc}^* \partial_r \psi_{sc} - \left(\partial_r \psi_{sc}^*\right)\psi_{sc}\right)(r^2 d\Omega) \xrightarrow[r\to\infty]{} v\left|f(\theta)\right|^2 d\Omega.$$

The partial-wave expansion

Neglecting spin for the moment, we use conservation of angular momentum to expand the wave function in partial waves of the orbital angular momentum,

$$\psi(r,\theta) = \sum_{l=0}^{\infty} u_l(r) P_l(\cos\theta).$$

The plane wave may be expanded as

$$e^{ikz} = \sum_{l=0}^{\infty} (2l+1) i^l j_l(kr) P_l(\cos\theta)$$

with

$$j_l(kr) = \frac{i}{2}\left(h_l^{(-)}(kr) - h_l^{(+)}(kr)\right) \qquad \text{where} \qquad h_l^{(\pm)}(kr) \xrightarrow[r\to\infty]{} (\mp i)^l \frac{e^{\pm ikr}}{kr}.$$

In analogy with the plane wave, we write

$$\psi(r,\theta) = \sum_{l=0}^{\infty} (2l+1) i^l \psi_l(r) P_l(\cos\theta)$$

where each of the partial waves satisfies the Schrödinger equation

$$\left(\frac{\partial^2}{\partial r^2} + k^2 - \frac{2\mu}{\hbar^2}U(r) - \frac{l(l+1)}{r^2}\right)\left(r\psi_l(r)\right) = 0.$$

More on the partial-wave expansion

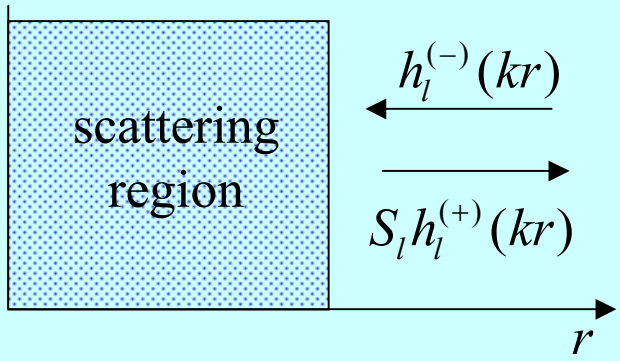

Outside the scattering region defined by the potential *U(r),* the wave function ψ_l(r) satisfies the same Schrödinger equation as the plane wave and must be a linear combination of the same incoming / outgoing waves $h_l^{(\pm)}(kr)$,

$$\psi_l(r) \to \frac{i}{2}\left(h_l^{(-)}(kr) - S_l h_l^{(+)}(kr)\right).$$

The incoming wave must be the same as that of the plane wave, so that the only difference with the plane wave is in the outgoing scattered wave.

Substituting in the partial wave expansion,

$$\psi(r,\theta) \to \sum_{l=0}^{\infty}(2l+1)i^l\left(j_l(kr) + \frac{S_l - 1}{2i}h_l^{(+)}(kr)\right)P_l(\cos\theta)$$

$$\to e^{ikz} + \frac{1}{2ik}\sum_{l=0}^{\infty}(2l+1)\left(S_l - 1\right)P_l(\cos\theta)\frac{e^{ikr}}{r},$$

so that

$$f(\theta) = \frac{1}{2ik}\sum_{l=0}^{\infty}(2l+1)\left(S_l - 1\right)P_l(\cos\theta) = \frac{4\pi}{2ik}\sum_{lm}\left(S_l - 1\right)Y_{lm}(\hat{r})Y_{lm}^*(\hat{k}).$$

Solving the scattering problem

How do we obtain the asymptotic form of the wave function,

$$\psi_l(r) \to \frac{i}{2}\left(h_l^{(-)}(kr) - S_l h_l^{(+)}(kr)\right)?$$

First, we fix a radius r_m, called the matching radius, that is beyond the range of the interaction.

The wave function inside the matching radius, ψ_{in}, is determined numerically, up to a multiplicative factor. Outside the matching radius, the wave function has the asymptotic form,

$$\psi_{l,ex}(r) = \frac{i}{2}\left(h_l^{(-)}(kr) - S_l h_l^{(+)}(kr)\right).$$

We require continuity of the wave function and its derivative at the matching radius.

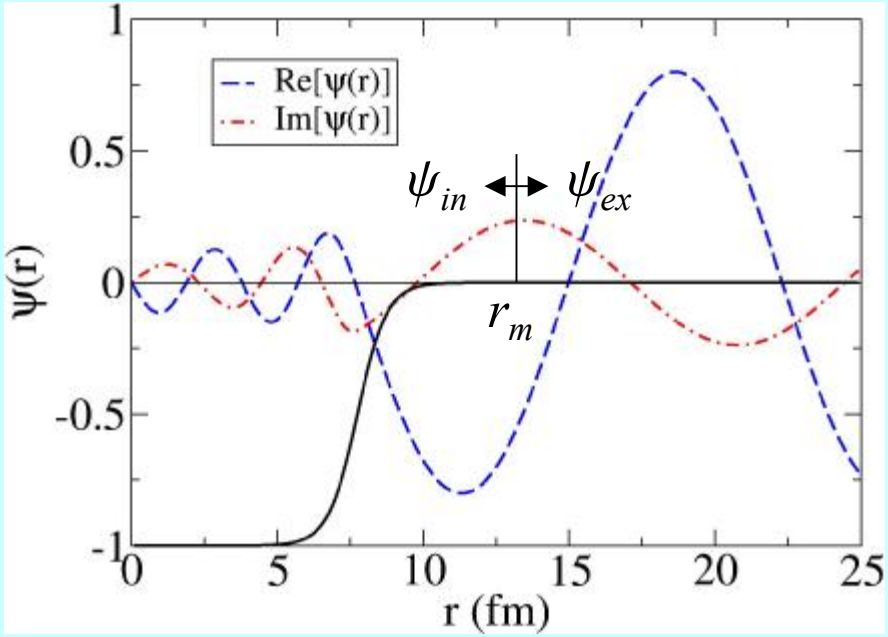

This gives us two equation in two unknowns, A_l and S_l,

$$A_l \psi_{l,in}(r_m) = \frac{i}{2}\left(h_l^{(-)}(kr_m) - S_l h_l^{(+)}(kr_m)\right)$$

and the derivative equation. We solve these for each value of l, stopping when S_l is sufficiently close to one.

Integrated cross sections

We obtain the elastic cross section by integrating over the differential one,

$$\sigma_{el} = 2\pi \int_0^{\pi} |f(\theta)|^2 \sin\theta d\theta = \frac{\pi}{k^2} \sum_{l=0}^{\infty} (2l+1) |S_l - 1|^2 .$$

We may calculate the absorption cross section by taking into account all of the flux entering and leaving the scattering region. Integrating the flux over a sphere whose radius tends to infinity, we have

$$\sigma_{abs} = -\frac{1}{v} \oint_S \vec{j} \cdot d\vec{S} = \frac{\pi}{k^2} \sum_{l=0}^{\infty} (2l+1) \left(1 - |S_l|^2\right).$$

The total cross section takes into account all flux lost from the incident plane wave, either by scattering or absorption,

$$\sigma_{tot} = \sigma_{el} + \sigma_{abs} = \frac{2\pi}{k^2} \sum_{l=0}^{\infty} (2l+1) \left(1 - \mathrm{Re}\, S_l\right).$$

The total cross section satisfies the optical theorem,

$$\sigma_{tot} = \frac{4\pi}{k} \mathrm{Im}\, f(\theta = 0^\circ).$$

Low-energy neutron scattering – a simple example

Because of the Coulomb barrier, only neutral particles can reach the nucleus in a low-energy scattering. At extremely low energies, the centripetal barrier keeps all but l=0, s-waves away from the nucleus.

Let us re-examine hard-sphere scattering in the case of low-energy neutron scattering.

Scattering from the hard sphere requires that the wave-function vanish at the radius of the sphere. The s-wave wave function is then

$$\psi_0(r) = \frac{i}{2kr}(e^{-ikr} - e^{-2ikR}e^{ikr}).$$

The S-matrix element is $S_0 = e^{2ikR}$.

The elastic cross section is

$$\sigma_{el} = 4\pi\frac{d\sigma}{d\Omega} = \frac{\pi}{k^2}\left|e^{-2ikR} - 1\right|^2.$$

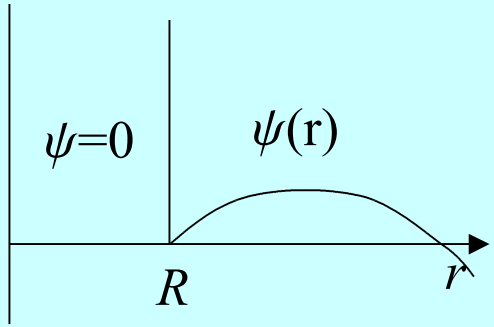

When $k\to 0$, the elastic cross section tends to a constant,

$$\sigma_{el} \xrightarrow[k\to 0]{} 4\pi R^2.$$

This is 4 times the classical cross section.

Low-energy neutron scattering -- resonances

Although the neutron-nucleus interaction is attractive, its rapid variation at the nuclear surface has the same effect on low energy neutrons as a hard-sphere does– the neutrons are reflected. Absorption also usually occurs, so that the total cross section is larger than the elastic one. However, if both the elastic scattering and absorption are prompt processes, one would expect them to vary slowly with energy. Behavior of this type can be seen on the low energy side of the figure.

The cross section of the figure also possesses a rapidly varying resonant component, a feature common to all low-energy neutron-nucleus systems.

The resonant contribution arises from scattering through a quasi-bound state (a compound nuclear state) of the neutron+nucleus.

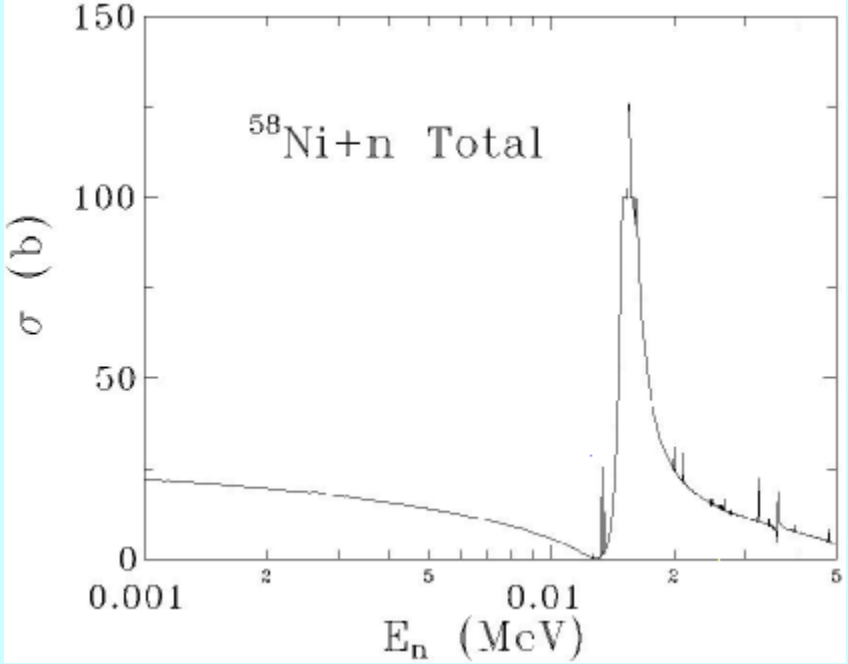

Direct and compound nuclear scattering

At low energies, neutron-nucleus scattering occurs either directly or through the quasi-bound compound nucleus states.

Direct scattering

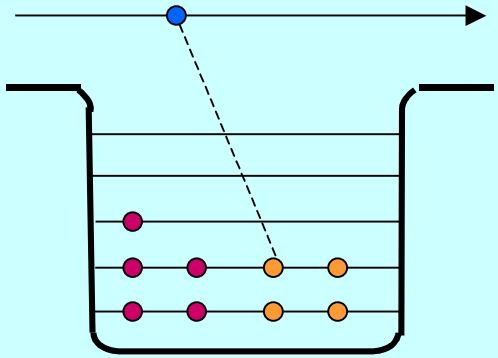

$\Delta t \sim 10^{-20} - 10^{-22}\,\mathrm{s}$

$\Delta E \Delta t \geq \hbar$

Compound nuclear scattering

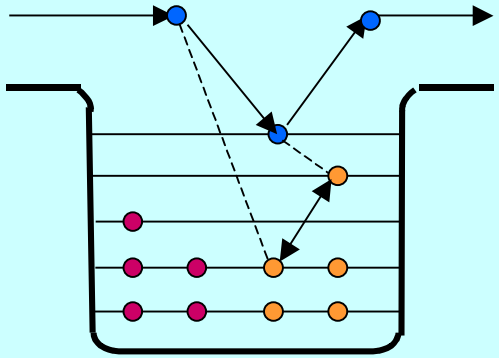

$\Delta t \sim 10^{-12} - 10^{-20}\,\mathrm{s}$

In a direct scattering, the incident neutron interacts with the average field of the nucleus. The duration of the collision is approximately the time it takes the neutron to cross the nucleus.

In a compound nuclear scattering, the incident neutron loses energy upon colliding with the nucleus and is trapped. After a fairly long interval, enough energy is again concentrated on one neutron to allow it to escape.

Formalities - I

To formally separate the direct and compound nucleu contributions, we assume that we can partition the space of states into two components:

$\mathcal{P}$ -- containing the continuum states, such as the n + ^{58}Ni ones, and

$\mathcal{Q}$ -- containing the quasi-bound states, such as the ground and excited states of ^{59}Ni (and any other states that we don't want in $\mathcal{P}$).

We define projection operators, P and Q, onto the subspaces with the properties

$$P^\dagger = P \qquad Q^\dagger = Q,$$
$$P^2 = P \qquad Q^2 = Q,$$
$$P + Q = 1$$

We then decompose the wave function into $\Psi = P\Psi + Q\Psi$, where $P\Psi$ is the continuum component and $Q\Psi$ the quasi-bound component of the wave function.

Formalities - II

Using P and Q, we decompose the Schrödinger equation, $(E - H)\,\Psi = 0$, into coupled equations for the two components of the wave function. We then write the solution for the $\mathcal{P}$-subspace component as,

$$P\Psi_c = \phi_c^{(+)} + (E^{(+)} - H_{PP})^{-1} V_{PQ} (E - H_{QQ} - W_{QQ})^{-1} V_{QP} \phi_c^{(+)}.$$

where the wave function $\phi_c^{(+)}$ satisfies the equation

$$(E - H_{PP})\phi_c^{(+)} = 0.$$

and

$$W_{QQ} \equiv V_{QP} (E^{(+)} - H_{PP})^{-1} V_{PQ} = V_{QP} \frac{P.P.}{E - H_{PP}} V_{PQ} - i\pi V_{QP} \delta(E - H_{PP}) V_{PQ}.$$

The prompt contribution to the scattering is contained in the wave function $\phi_c^{(+)}$ and in the $\mathcal{P}$-subspace propagator. The compound nucleus term takes into account passage through the continuum through the W_{QQ} term in the $\mathcal{Q}$-subspace propagator. The open channels in the $\mathcal{P}$ subspace make a negative imaginary contribution to W_{QQ}, leading to poles of the the wave function in the lower half of the complex energy plane.

Low-energy neutron scatterng -- resonances

We now apply the expression for the $\mathcal{P}$-subspace wave function,

$$P\Psi_c = \phi_c^{(+)} + (E^{(+)} - H_{PP})^{-1} V_{PQ} (E - H_{QQ} - W_{QQ})^{-1} V_{QP} \phi_c^{(+)},$$

to s-wave neutron scattering, for which,

$$\psi_0(r) = \frac{i}{2kr}(e^{-ikr} - S_0 e^{ikr}),$$

outside the range of the interaction. (We continue to neglect the spin of the neutron.)

After a bit of work, we can approximate the S-matrix of the $\mathcal{P}$-subspace wave function in a multi-level Breit-Wigner form (among others) as

$$S_{0,ab} = e^{-i(\phi_a + \phi_b)} \left(\delta_{ab} - i \sum_\mu \frac{g_{\mu a} g_{\mu b}}{E - \varepsilon_\mu + i\Gamma_\mu / 2} \right),$$

where ϕ_a and ϕ_b are the initial and final channel phase shifts and the amplitudes $g_{\mu c}$ characterize the coupling of the compound state μ to the continuum channel c, with $\Gamma_\mu = \sum_c g_{\mu c}^2$.

The phase shifts vary slowly with the energy while the resonance sum varies quickly.

Low-energy neutron scattering – cross sections

The cross sections directly related to the elastic S-matrix element are the elastic, absorption and total ones,

$$\sigma_{el} = \frac{\pi}{k^2}\left|S_{0,aa} - 1\right|^2, \qquad \sigma_{abs} = \frac{\pi}{k^2}\left(1 - \left|S_{0,aa}\right|^2\right),$$

and

$$\sigma_{tot} = \sigma_{el} + \sigma_{abs} = \frac{2\pi}{k^2}\left(1 - \mathrm{Re}\, S_l\right).$$

The absorption cross section is non-zero when non-elastic channels, such as γ emission or fission, remove flux from the compound nucleus. The cross sections for these take the form

$$\sigma_{ac} = \frac{\pi}{k^2}\left|S_{0,ca}\right|^2.$$

The total flux is conserved,so that

$$\sigma_{abs} = \sum_{c \neq a} \sigma_{ca} \qquad \text{and} \qquad \sigma_{tot} = \sigma_{el} + \sigma_{abs}.$$

The elastic cross section is well described at energies below the resonance region by a hard-sphere cross section of $4\pi R^2$.

From resonances to fluctuations

At low energies, the resonance expression for the S-matrix permits the separation of the direct and compound contributions to cross sections. However, as the energy increases, both the resonance widths and the density of compound nucleus states increase, so that the resonances eventually overlap and can no longer be distinguished. The cross section fluctuates rapidly, as in the figure, but the fluctuations, called Ericson fluctuations, cannot be attributed to individual resonances.

It is in this context that the optical model plays a fundamental role. The objective of the model is to describe just the prompt, direct reactions in a collision. To this end, one defines the optical potential as the potential that furnishes the energy-averaged (short time) scattering amplitudes.

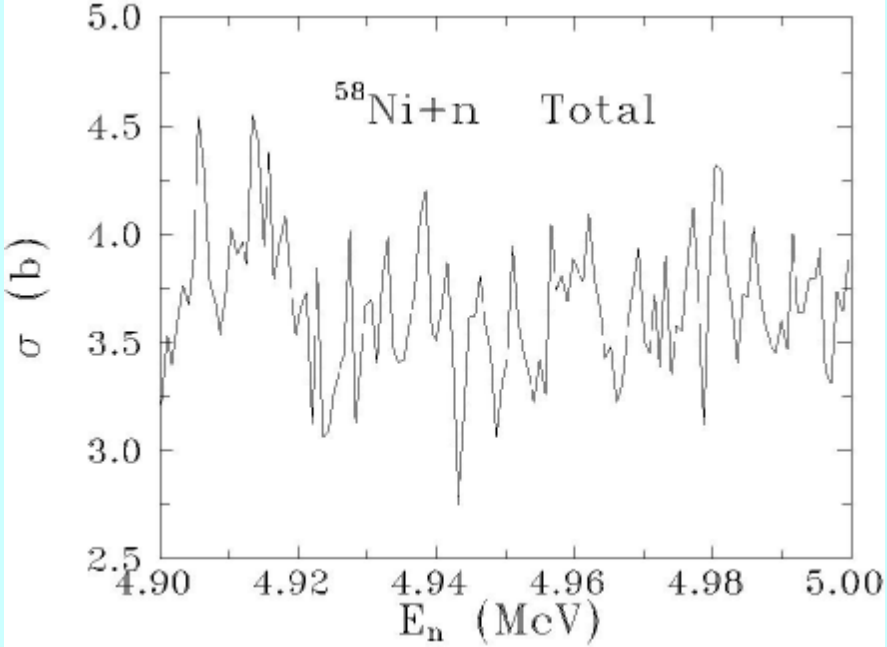

Energy averaging and the optical potential

To obtain the optical potential, we begin by calculating the energy average of the $\mathcal{P}$-subspace wave function, which depends linearly on the scattering amplitude. After rewriting the wave function in the form of an equation, we will obtain an expression for the optical potential.

The energy average of the $\mathcal{P}$-subspace wave function may be written directly,

$$\left\langle P\Psi_c \right\rangle = \phi_c^{(+)} + (E^{(+)} - H_{PP})^{-1} V_{PQ} \left\langle 1/e_{QQ} \right\rangle V_{QP} \phi_c^{(+)}.$$

since the only rapidly varying quantity in the wave function is

$$e_{QQ} = E - H_{QQ} - W_{QQ}.$$

By multiplying by (E-H_{PP}) as well as solving formally for $\phi_c^{(+)}$ and substituting, we can write a Schrödinger-like equation for $\langle P\Psi_c \rangle$,

$$\left(E - H_{PP} - V_{PQ} \frac{1}{\left\langle 1/e_{QQ} \right\rangle^{-1} + W_{QQ}} V_{QP} \right) \left\langle P\Psi_c \right\rangle = 0.$$

The optical potential is then

$$U_{opt} = V_{PP} + V_{PQ} \frac{1}{\left\langle 1/e_{QQ} \right\rangle^{-1} + W_{QQ}} V_{QP}$$

Performing the energy average

To conclude the derivation of the optical potential, we must calculate $\langle 1/e_{QQ}\rangle$. Although there are many ways to perform the average, the simplest is to average over a normalized Lorentzian density,

$$\left\langle 1/e_{QQ}\right\rangle = \int dE_0 \, \frac{\rho(E,E_0)}{E_0 - H_{QQ} - W_{QQ}}$$

where

$$\rho(E,E_0) = \frac{\Delta}{2\pi}\frac{1}{(E-E_0)^2 + \Delta^2/4}.$$

Assuming that $1/e_{QQ}$ has no poles in the upper half of the complex E plane (causality), we can perform the integral by closing the contour in the UHP to find

$$\left\langle 1/e_{QQ}\right\rangle = (E + i\Delta/2 - H_{QQ} - W_{QQ})^{-1}$$

so that

$$U_{opt} = V_{PP} + V_{PQ}\frac{1}{E - H_{QQ} + i\Delta/2}V_{QP}$$

The optical potential is energy-dependent, non-local and complex. Its imaginary part is negative, resulting in a potential that is absorptive. The absorption accounts for the flux that is lost to the Q-subspace.

Low-energy neutron scattering – optical potential

One finds for the low-energy neutron s-wave S-matrix element $S_0 = e^{-2ik\rho}$, where ρ is a complex scattering length. $R = |\rho|$ is called the scattering radius.

The resulting elastic cross section tends to a constant as the energy tends to zero, while the absorption and total cross sections diverge at small energy as *1/k*.

We have, as $k \to 0$,

$$\sigma_{el} = 4\pi \frac{d\sigma}{d\Omega} \to 4\pi R^2,$$

$$\sigma_{abs} \to -\frac{4\pi}{k} \operatorname{Im} \rho \left(1 + 2k \operatorname{Im} \rho\right),$$

and

$$\sigma_{tot} = \sigma_{el} + \sigma_{abs}.$$

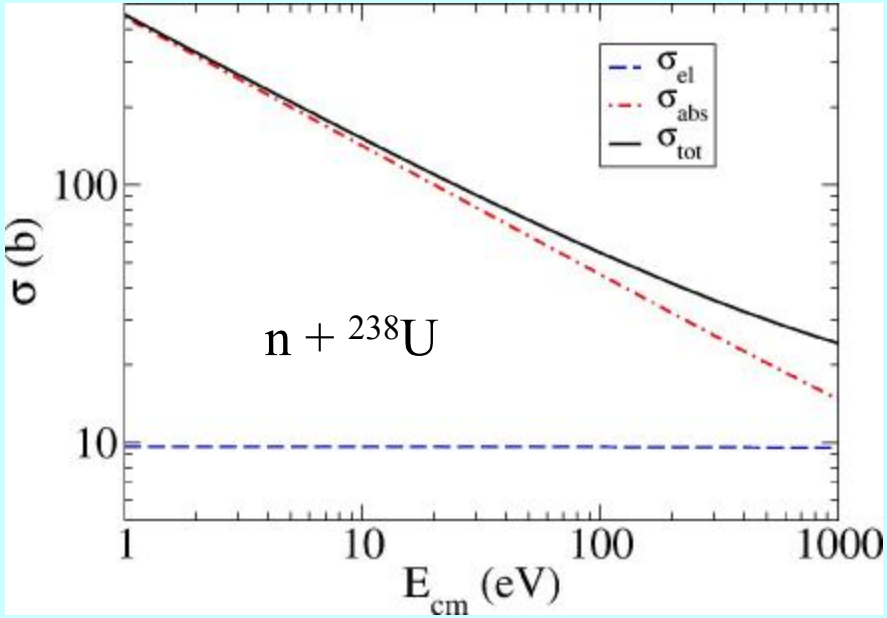

Experimental significance

An optical model calculation furnishes a wave function and a scattering amplitude that should describe the prompt part of the scattering. The S-matrix that results is an energy-averaged one. We could write the S-matrix before averaging as

$$\mathfrak{S}_0 = S_0 + S_{0,fluc}, \quad \text{with} \quad \langle S_{0,fluc} \rangle = 0, \quad \text{so that} \quad \langle \mathfrak{S}_0 \rangle = \langle S_0 \rangle.$$

The energy-averaged total cross-section is just the optical one,

$$\sigma_{tot} = \frac{2\pi}{k^2}\left(1 - \mathrm{Re}\langle \mathfrak{S}_0 \rangle\right) = \frac{2\pi}{k^2}\left(1 - \mathrm{Re}\, S_0\right),$$

since it is linear in the S-matrix.

However, the energy-averaged elastic and absorption cross sections are

$$\sigma_{el} = \frac{\pi}{k^2}\left\langle \left|\mathfrak{S}_0 - 1\right|^2 \right\rangle = \frac{\pi}{k^2}\left|S_0 - 1\right|^2 + \frac{\pi}{k^2}\left\langle \left|S_{0,fluc}\right|^2 \right\rangle$$

and

$$\sigma_{abs} = \frac{\pi}{k^2}\left\langle 1 - \left|\mathfrak{S}_0\right|^2 \right\rangle = \frac{\pi}{k^2}\left(1 - \left|S_0\right|^2\right) - \frac{\pi}{k^2}\left\langle \left|S_{0,fluc}\right|^2 \right\rangle.$$

Only the total optical cross section may be compared with the experimental one.

The s-wave strength function

If we average the resonance expression for the elastic S-matrix,

$$S_{0,aa} = e^{-2i\phi_a}\left(1 - i\sum_{\mu}\frac{\Gamma_{\mu a}}{E-\varepsilon_{\mu}+i\Gamma_{\mu}/2}\right), \qquad \text{where} \quad \Gamma_{\mu a} = g_{\mu a}^2,$$

over the Lorentzian that was used to obtain the optical potential, we find

$$\bar{S}_{0,aa} = e^{-2i\phi_a}\left(1 - i\sum_{\mu}\frac{\Gamma_{\mu a}}{E-\varepsilon_{\mu}+i\Delta}\right) \approx e^{-2i\phi_a}\left(1 - \frac{\pi\bar{\Gamma}_n}{D}\right),$$

where $\bar{\Gamma}_n$ is the average neutron width and D the average s-wave resonance spacing. Since the average is the same as that of the optical potential, the average S-matrix should be the same as the optical one. In particular, we expect

$$1 - \left|S_0\right|^2 \approx 2\pi\frac{\bar{\Gamma}_n}{D}$$

when $\bar{\Gamma}_n << D$. We define the strength function as

$$s_0 = \frac{\bar{\Gamma}_n}{D}\left(\frac{E_0}{E_{cm}}\right)^{1/2} \approx \frac{1}{2\pi}\left(\frac{E_0}{E_{cm}}\right)^{1/2}\left(1 - \left|S_0\right|^2\right)$$

where E_0 is usually taken to be 1 eV. The factor of $\sqrt{E_{cm}}$ cancels the energy dependence of the neutron partial width.

Strength functions and SPRT

The s-wave strength function may be obtained from experimental data, either from measurements of the total cross section or from averages over resonances. When compared to optical model calculations, the agreement is quite good. The two peaks in the s-wave strength function occur in the regions where the 3s1/2 and 4s1/2 neutron shell-model orbitals are becoming bound and have a large overlap with continuum states.

A p-wave strength function may also be associated with p-wave absorption and extracted from data. The two strength functions, together with the scattering radius and the total cross section, may be used to fit optical model parameters at low energy. This is known as the SPRT method.

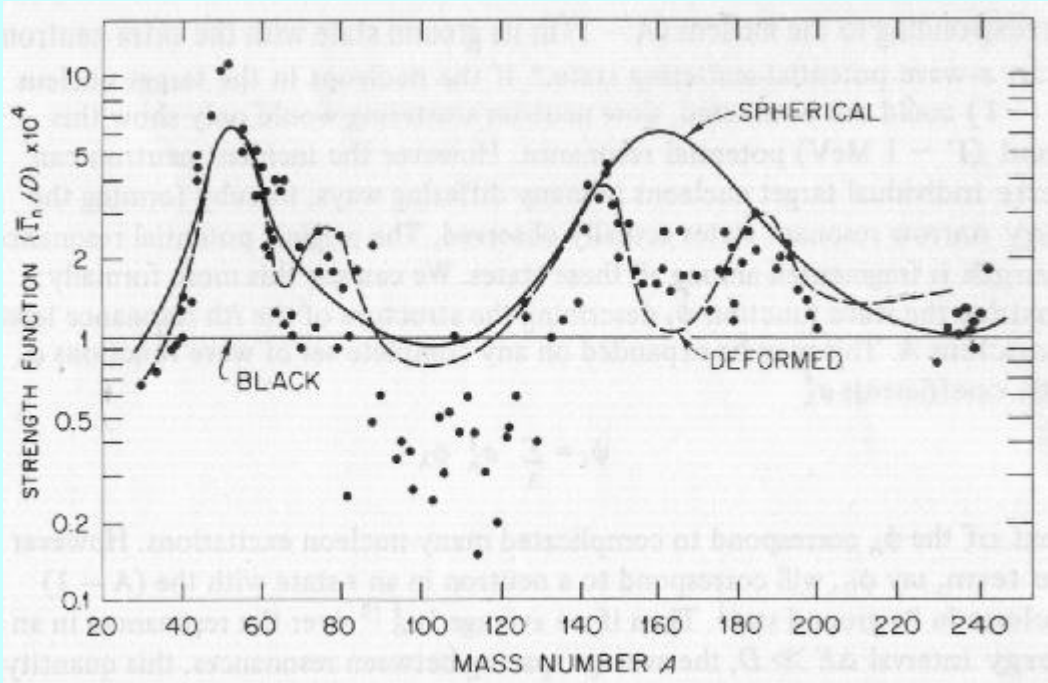

Higher partial waves

The angular distribution for a pure s-wave is obviously constant. As the energy increases, more partial waves participate in the scattering and the angular distribution becomes more forward peaked.

The highest partial wave contributing to the scattering may be crudely estimated as $l_{max} \approx kR$. For n+^{238}U at an energy of 1 MeV, this gives $l_{max} \approx 1.6$.

An important auxiliary quantity determined in an optical model calculation is the transmission coefficient, $T_l = 1 - |S_l|^2$, which is used to calculate the fluctuating contribution to the cross sections. The transmission coefficient measures the fraction of flux that is absorbed from each partial wave.

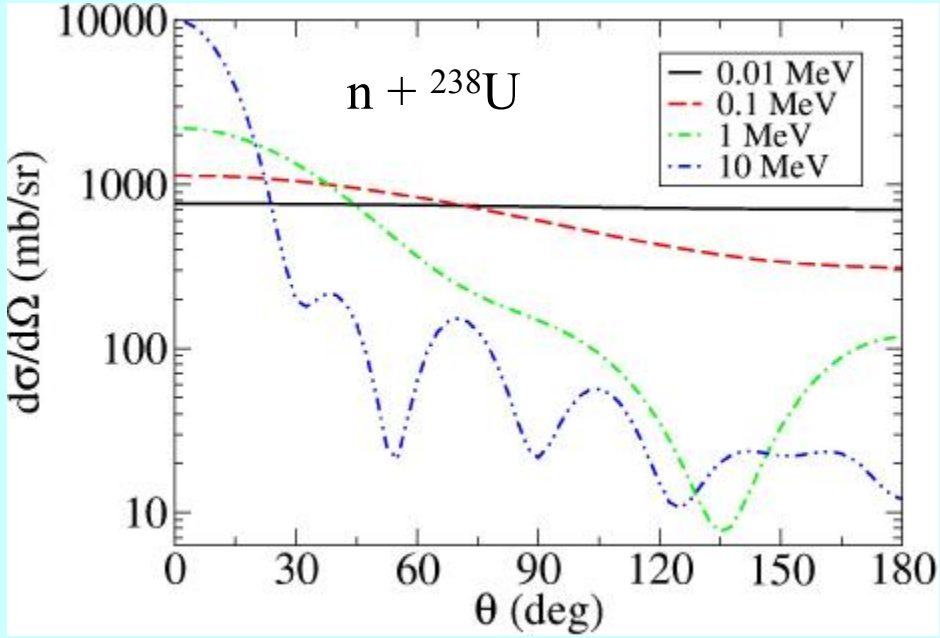

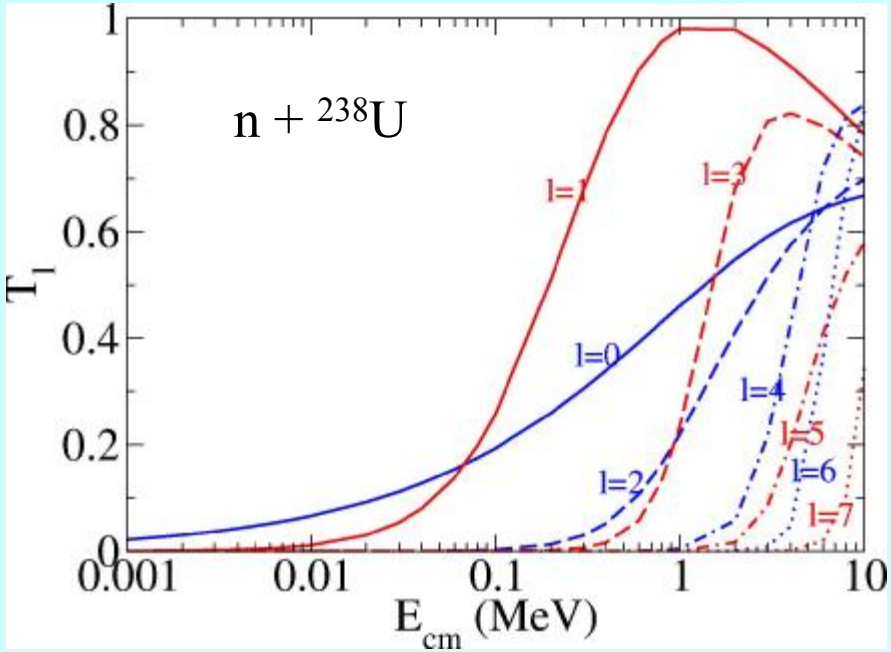

The partial wave expansion for charged particles

The difference between the partial wave expansion for neutral and charged particles is the long-range Coulomb potential. Rather than consider a plane wave, one must consider a Coulomb wave,which contains an additional logarithmic phase. The wave function may be expanded as

$$\psi_c = \frac{1}{kr}\sum_{l=0}^{\infty}(2l+1)i^l e^{i\sigma_l} F_l(kr) P_l(\cos\theta),$$

with

$$F_l(kr) = \frac{i}{2}\left(e^{-i\sigma_l} H_l^{(-)}(kr) - e^{i\sigma_l} H_l^{(+)}(kr)\right)$$

where the σ_l are the Coulomb phase shifts and

$$H_l^{(\pm)}(kr) \xrightarrow[r\to\infty]{} \left(\mp i\right)^l e^{\pm i\left(kr - \eta \ln 2kr\right)} \quad \text{with} \quad \eta = ka_0.$$

One may proceed as before to extract the scattering amplitude as

$$f(\theta) = f_C(\theta) + \frac{1}{2ik}\sum_{l=0}^{\infty}(2l+1)e^{2i\sigma_l}\left(S_l - 1\right)P_l(\cos\theta).$$

where

$$f_C(\theta) = -\frac{\eta}{2k\sin^2\theta/2}\exp\left[-i\eta\ln\left(\sin^2\theta/2\right) + 2i\sigma_0\right].$$

The quantum Coulomb scattering cross section is identical to the classical one.

Proton scattering

The angular distribution for proton scattering on 58Ni at 1 MeV is a pure Coulomb one. Even at 4 MeV, the difference from the pure Coulomb angular distribution appears small. At 10 MeV, substantial deviations have appeared.

Nuclear effects are more easily distinguished in the transmission coefficients. They support the observation that the scattering is purely Coulomb at 1 MeV. However, at 4 MeV, 40% of the s-wave and about 10% of the p- and d-wave have been absorbed. Angular momenta through l=4 contribute at 10 MeV.

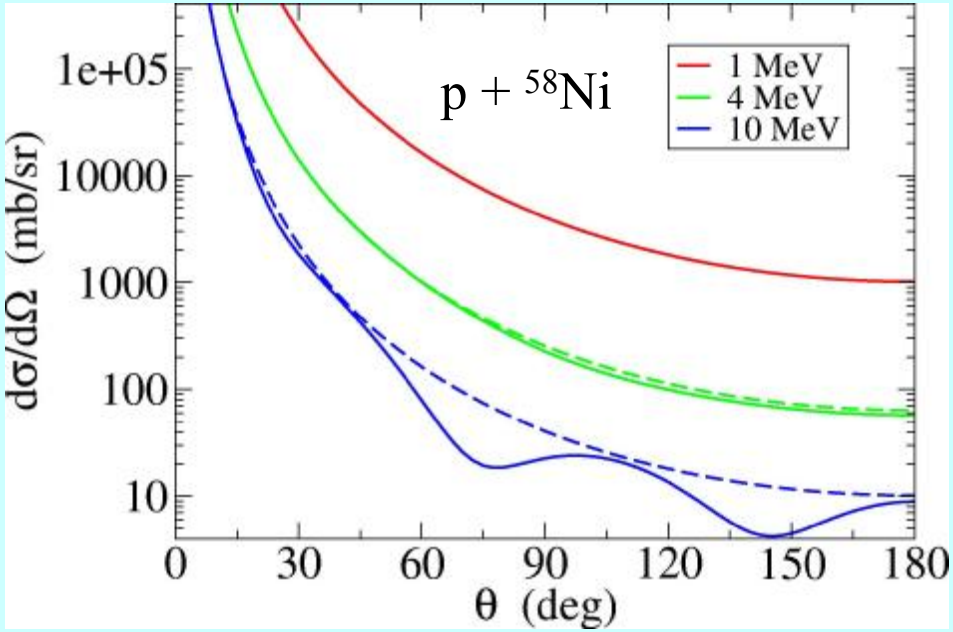

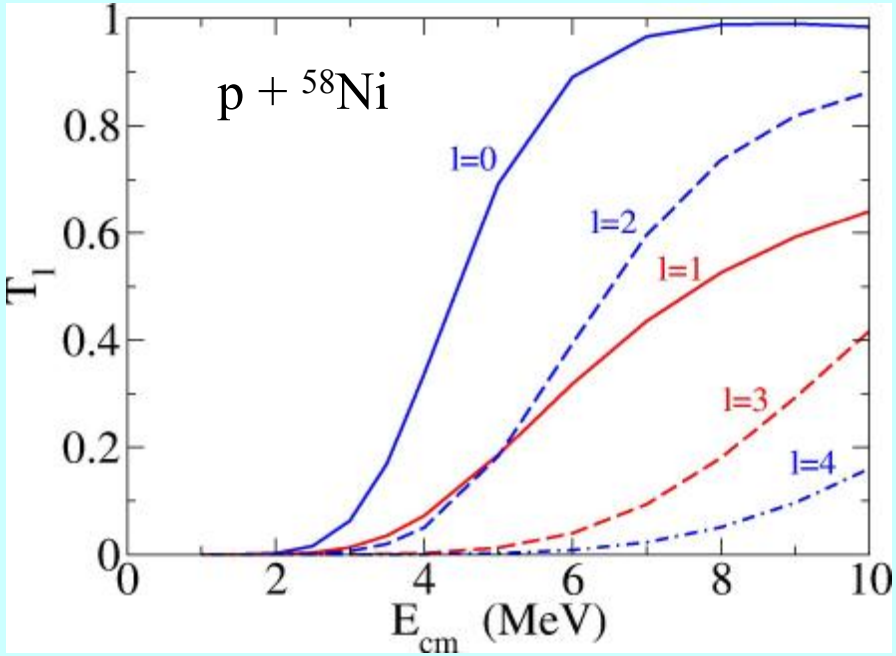

The optical potential

We obtained a formal expression for the optical potential,

$$U_{opt} = V_{PP} + V_{PQ} \frac{1}{E - H_{QQ} + i\Delta/2} V_{QP}$$

by rewriting the energy-average of the continuum component of the wave function as an equation for itself. We observed that this potential is complex, non-local and energy-dependent.

A good deal of work has been done to calculate the optical potential from first principles. These potentials are usually non-local, except at very high energies, which tends to complicate their use.

Phenomenological optical potentials are normally used to fit and compare with experimental data. These potentials are usually taken to be local. However, their geometrical characteristics and the general trend of their energy dependence are quite similar to those of microscopic potentials. They can furnish insight into what one should expect of a microscopic potential. After all, both potentials are trying to describe the same physical processes.

The phenomenological optical potential

Empirical optical potentials are determined by adjusting a limited set of parameters to the data on hand. Over the years, a standard form of the potential has evolved, which permits the parametrization of the scattering of most light particles (n, p, d, t, 3He, or α) from most nuclei. This is

$$
\begin{aligned}
U_{opt}(r) = \quad & V_C(r) && \text{a Coulomb term,} \\
& -Vf_V(r) \; - \; iWf_W(r) && \text{volume terms,} \\
& +V_S g_V(r) - iW_S g_W(r) && \text{surface terms,} \\
& -d_{so}\vec{l}\cdot\vec{\sigma}\left(V_{so}h_V(r) - iW_{so}h_W(r)\right), && \text{spin-orbit terms}
\end{aligned}
$$

where the spin-orbit constant is $d_{so} = \left(\hbar / m_\pi c\right)^2 \approx 2 \text{ fm}^2$.

The Coulomb potential is usually taken to be the interaction of a point charge with a uniformly-charged sphere of radius R_c=1.25*A$^{1/3}$ (fm),

$$
V_C(r) = \begin{cases} \dfrac{Z_P Z_T e^2}{2R_C}\left(3 - (r/R_C)^2\right) & r < R_C \\ \dfrac{Z_P Z_T e^2}{r} & r > R_C \end{cases}
$$

The volume terms of the optical potential

The volume terms are usually taken to be of Wood-Saxon form,

$$f_i(r) = \frac{1}{1+\exp\left[(r-R_i)/a_i\right]} \qquad i = V, W,$$

where R_i and a_i are the radii and diffusivities of the two terms.

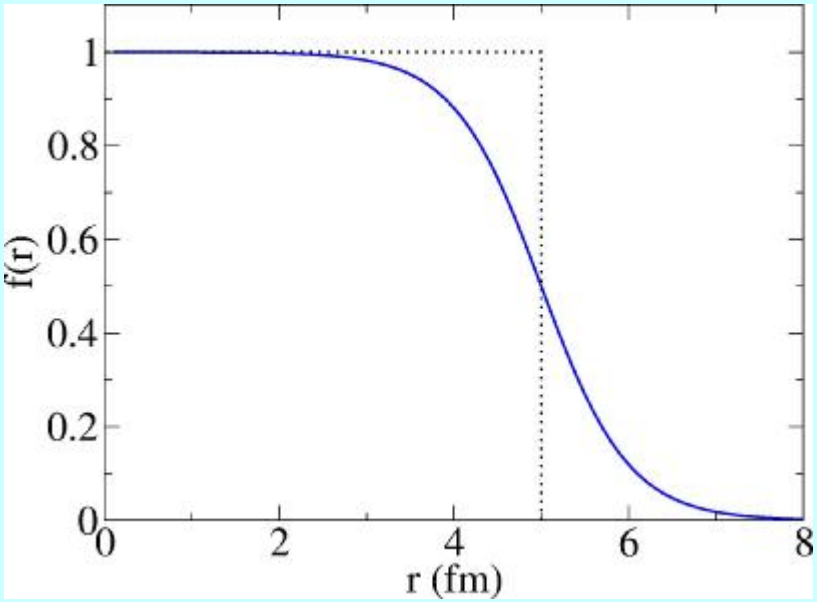

The Wood-Saxon form is quite similar to the nucleon density of a saturated nucleus (A>30).

The real volume potential reflects the average interaction of the projectile with the nucleons of the target. The strength of the real volume potential is roughly proportional to the mass of the projectile and and decreases with energy, in agreement with nuclear mean field calculations.

The imaginary volume potential takes into account the loss of projectile flux due to collisions with the nucleons in the target. It is zero at low energy, below the threshold for single-particle excitations, and increases with energy as the phase space of single-particle modes increases.

The surface terms of the optical potential

The surface terms are usually taken to be either the derivative of a Wood-Saxon,

$$g_i(r) = -4a_i \frac{d}{dr} f_i(r) = 4 \frac{\exp\left[(r-R_i)/a_i\right]}{\left(1+\exp\left[(r-R_i)/a_i\right]\right)^2} \quad i = V, W,$$

or a Gaussian,

$$g_i(r) = \exp\left[(r-R_i)^2/a_i^2\right] \quad i = V, W.$$

The two are practically indistinguishable when a_G=2.21 a_{WS}.

The imaginary surface term takes into account the absorption due to the excitation of low-energy collective modes, which have their couplings concentrated on the surface.

A real surface term can result from the same coupling but can also be explained using a dispersion relation.

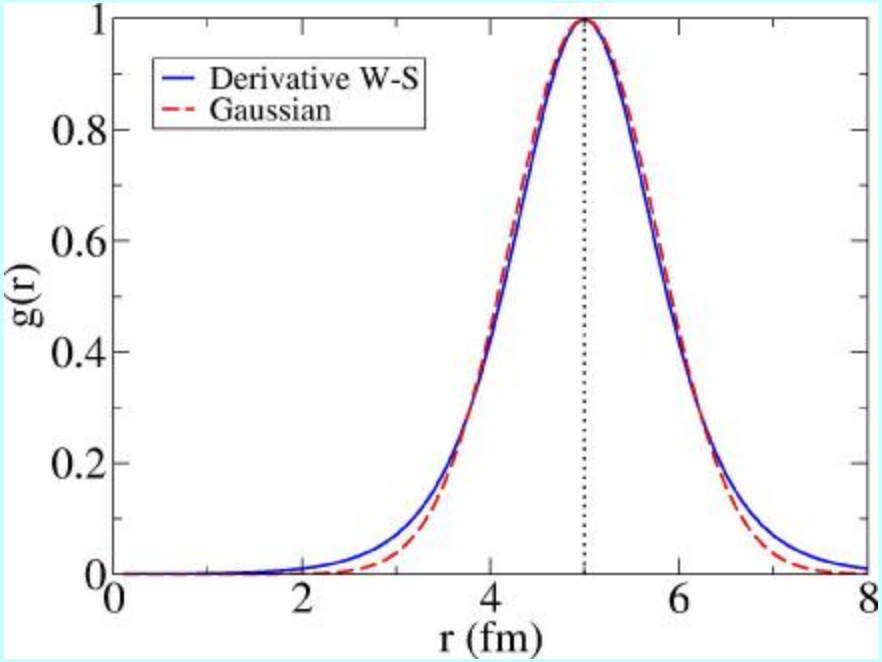

The spin-orbit terms of the optical potential

The spin-orbit terms are taken to have a Thomas form factor,

$$h_i(r) = -\frac{1}{r}\frac{d}{dr} f_i(r) = \frac{1}{r a_i} \frac{\exp\left[(r - R_i)/a_i\right]}{\left(1 + \exp\left[(r - R_i)/a_i\right]\right)^2} \qquad i = V, W.$$

The spin-orbit interaction also acts between the bound states of a nucleus, where it increases the binding of the $j=l+½$ levels and decreases the binding of the $j=l$-1/2 levels.

The Thomas form factor and the spin-orbit potential itself are obtained (for spin ½) when the Dirac equation with Wood-Saxon potentials is reduced to an equivalent Schrödinger equation. The spin-orbit interaction is thus another manifestation of the volume interaction of the projectile with the nucleons of the target.

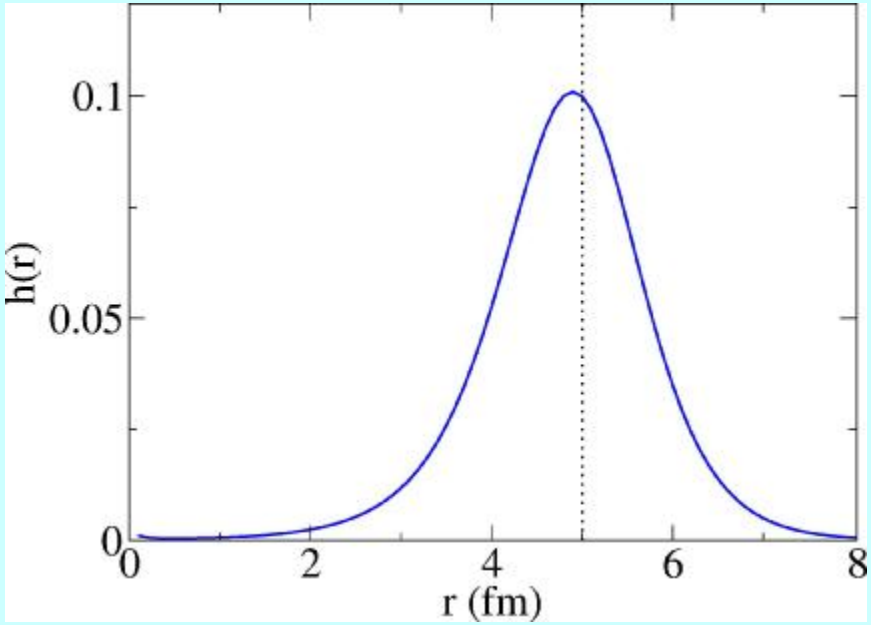

Optical potential parameters

The phenomenological optical potential is thus parametrized in terms of a set of potential strengths and corresponding geometrical parameters.

The best modern reference for optical potential parameters is the Reference Input Parameter Library (RIPL), available both online and in CD from the Internationational Atomic Energy Agency.

For nucleons, typical values of the potential strengths are

$$V \approx (45-55) \text{ MeV} - (0.2-0.3)E,$$

$$W_s \approx (2-7) \text{ MeV} - (0.1-0.3)E \qquad E < 8-10 \text{ MeV},$$

$$V_{so} \approx (4-10) \text{ MeV}.$$

Above 8-10 MeV, W_s is usually constant or slightly decreasing. V_s and W_{so} can normally be taken to be zero as can W below about 10 MeV. Above about 10 MeV, W is constant or slightly increasing.

The radii R_i take on values $R_i = r_i A_T^{1/3}$ with the reduced radii in the range $r_i \approx 1.2 - 1.3$ fm. The diffusivities are normally in the range $a_i \approx 0.4 - 0.7$ fm.

Fairly wide ranges of the parameters V, R_V, W_s and a_s result in equally good fits if VR_V^2 and $W_s a_s$ remain constant. These are potential ambiguities.

The microscopic optical potential -- I

Microscopic optical potentials attempt to describe the projectile-target interaction in terms of nucleon-nucleon interactions, such as these representing the first few terms in nucleon-nucleus interaction.

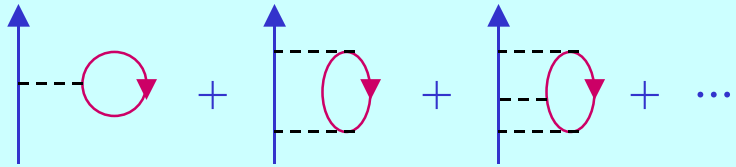

A systematic method for summing the most important terms is provided by the self-consistent Brueckner approximation. The Brueckner $\mathfrak{G}$-matrix is calculated by summing repeated interactions, taking into account effects of the nuclear medium.This calculation is usually performed in infinite nuclear matter, for simplicity.

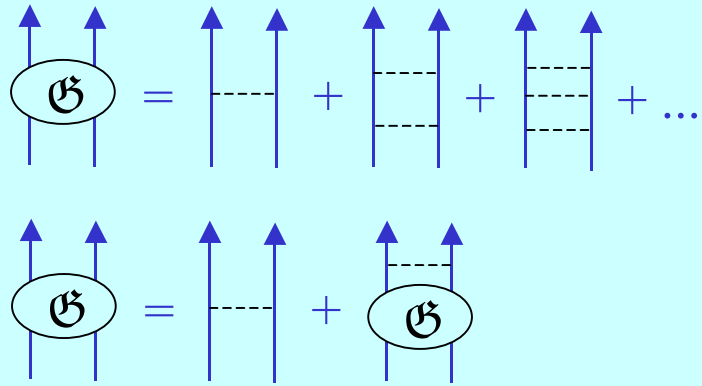

The $\mathfrak{G}$-matrix is then folded over the target nucleon density to obtain the optical potential *U*. Self-consistency requires that the target density be obtained with the same potential.

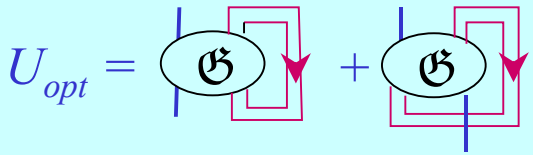

The microscopic optical potential -- II

The microscopic optical potential possesses a direct term and an exchange term. The exchange term is non-local and both are energy-dependent. The exchange term is often approximated as a local term with an additional energy-dependence (JLM).

U_{opt} = 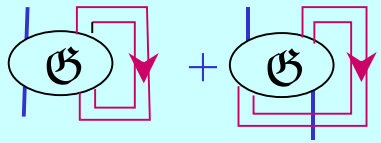 +

$= U_d + U_{ex}$

At high energy, the microscopic optical potential reduces to the impulse approximation potential, obtained by folding the two-nucleon *t*-matrix with the target density -- the $t\rho$ approximation.

The figure compares experimental reaction cross sections for ^{12}C, ^{28}Si, ^{56}Fe ^{90}Zr and ^{208}Pb, in ascending order, with microscopic optical model calculations by Amos and Karataglidis, nucl-th/0202050.

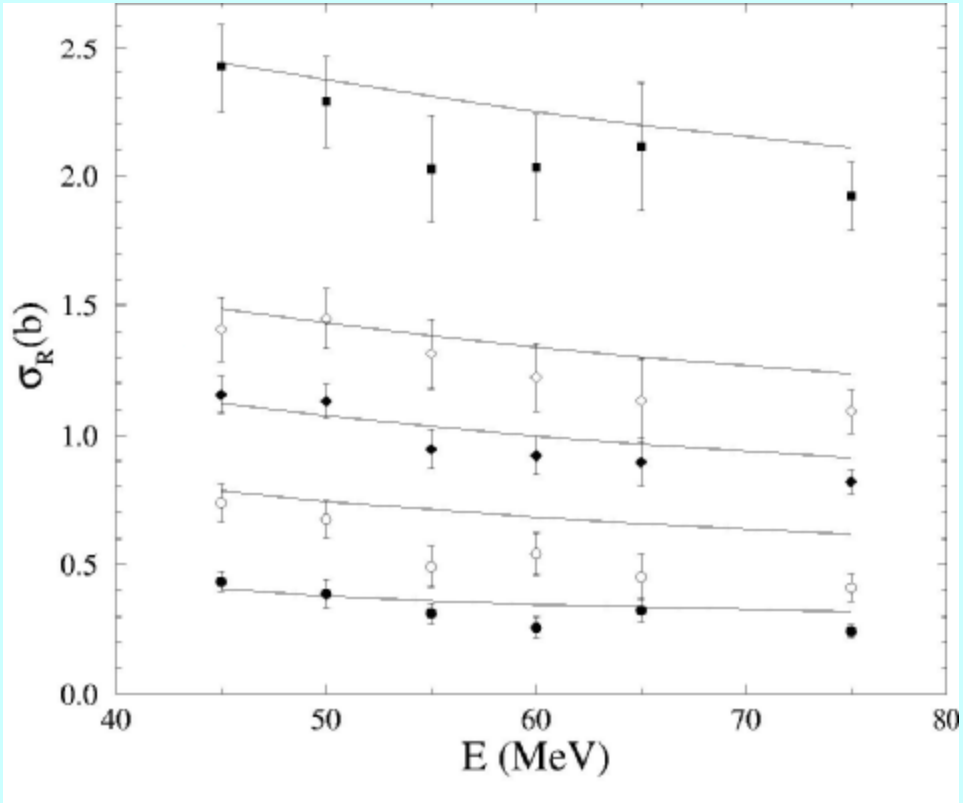

The microscopic potential at low energy

Formally, we derived the optical potential by considering the scattering in a subspace $\mathcal{P}$ of the space of states and then energy-averaged to smooth the dependence on the remaining subspace of states $\mathcal{Q}$. We obtained

$$U_{opt} = V_{PP} + V_{PQ} \frac{1}{E - H_{QQ} + i\Delta/2} V_{QP}.$$

In the microscopic optical potential, the division into $\mathcal{P}$ and $\mathcal{Q}$ subspaces is no longer transparent. It is there, contained in the $\mathfrak{G}$-matrix, but in terms of nucleon-nucleon scattering rather than nucleon-nucleus scattering. We would thus expect that the microscopic potential does not take into account the collective effects that are often important at low energies. We might consider decomposing the optical potential at low energies (using a local approximation) as

$$U_{opt}(r,E) = U_{sp}(r,E) + U_{coll}(r,E),$$

where U_{sp} is the microscopic potential and U_{coll} is the remainder, which we might attribute to collective effects. At low energies, $U_{sp}(r,E) \approx V_{HF}(r,E)$. At high energy, we expect that $U_{coll}(r,E) \to 0$.

Dispersion relations

Because of causality, the optical potential should have no singularities in the upper half-energy plane. We may then write

$$\oint dE' \frac{U_{coll}(r,E')}{E'-E} = 0,$$

which we may rewrite as

$$\text{P.P.}\int dE' \frac{U_{coll}(r,E')}{E'-E} = i\pi U_{coll}(r,E)$$

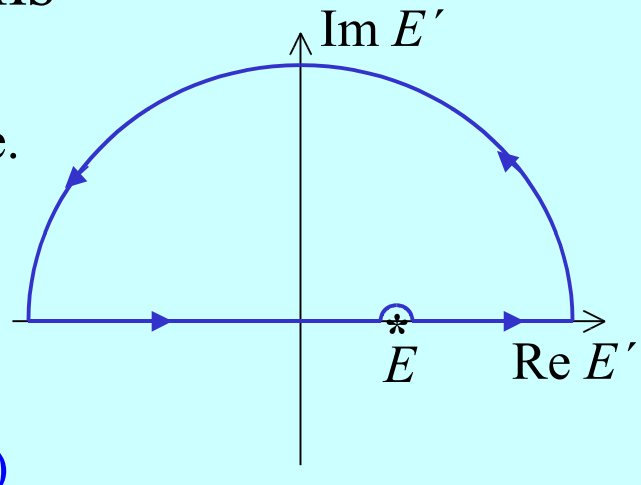

Separating U_{coll} into its real and imaginary parts, $U_{coll} = \Delta V + i\,W$, we have

$$\Delta V(r,E) = \text{P.P.}\frac{1}{\pi}\int dE' \frac{W(r,E')}{E'-E}$$

At low energy, $U_{opt} \approx V_{HF} + \Delta V + i\,W$.

The effect of ΔV is seen as a strengthening in the real part of the optical potential at low energy relative to the linear dependence expected of V_{HF}.

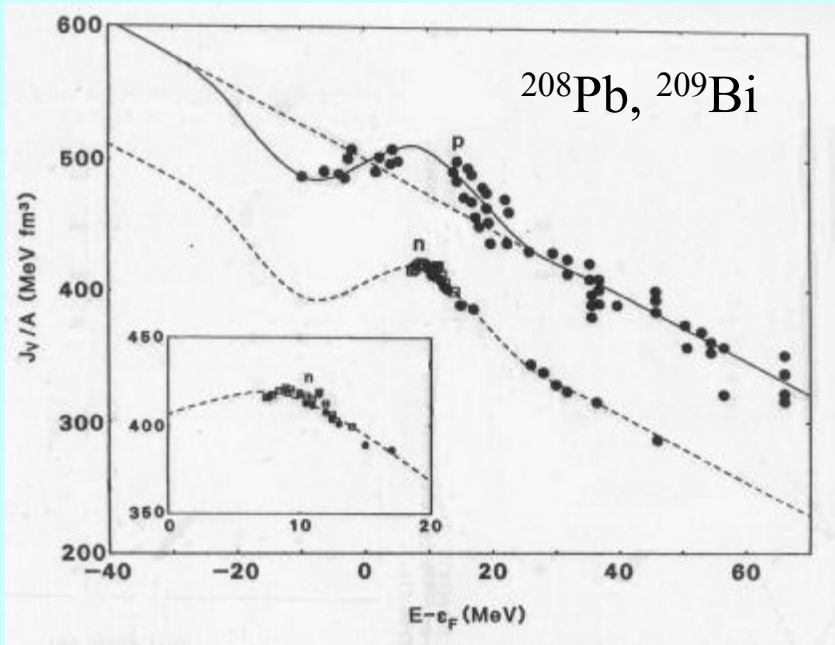

(Finlay and Petler, Opt. Model 1986)

The single-channel optical model -- spin

Because of the spin-orbit interaction, a rigorous treatment of neutron or proton scattering requires that the spin be included in the calculation. To do this, one performs the partial wave expansion of the scattering wave function (spin s) as

$$\Psi = \frac{4\pi}{kr}\sum_{ljn} i^l e^{i\sigma_l}\psi_l^j(r)\mathcal{Y}_{ls}^{jn}(\hat{r})\mathcal{Y}_{ls}^{jn\dagger}(\hat{k}),$$

in terms of the spin-angular functions,

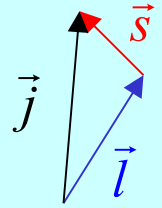

$$\mathcal{Y}_{ls}^{jn}(\hat{r}) = i^l\sum_{m\nu}\left\langle lms\nu \middle| j\,n\right\rangle Y_{lm}(\hat{r})\left|s\nu\right\rangle,$$

where l and j are the orbital and total angular momenta and $|s\nu\rangle$ is a spin eigenvector. In the expansion, σ_l is the Coulomb phase shift, $\hat{r}$ denotes the angular variables and $\hat{k}$ the direction of the incident momentum. The spin-angular functions are vectors with components labeled by ν, the projection of the spin.

Because of angular momentum and parity conservation, the equations for the $\psi_l^j(r)$ uncouple. They can then be solved as before and the asymptotic behavior of the resulting wave function analyzed to extract the scattering amplitude.

The scattering amplitude -- spin

The scattering amplitude

$$f(\theta) = f_C(\theta)\mathbf{1} + \frac{4\pi}{2ik}\sum_{ljn} e^{2i\sigma_l}\left(S_l^j - 1\right)\mathcal{Y}_{ls}^{jn}(\hat{r})\mathcal{Y}_{ls}^{jn\dagger}(\hat{k}),$$

with $f_C(\theta)$ the Coulomb scattering amplitude, is now a matrix, $f_{\nu\nu'}(\theta)$, with matrix elements labeled by the spin projections ν and ν'.

For particles of spin ½,

$$f(\theta) = \begin{pmatrix} A(\theta) & B(\theta) \\ B(\theta) & A(\theta) \end{pmatrix}$$

where

$$A(\theta) = f_C(\theta) + \frac{1}{2ik}\sum_l e^{2i\sigma_l}\left[(l+1)\left(S_l^{l+1/2} - 1\right) + l\left(S_l^{l-1/2} - 1\right)\right]P_l(\cos\theta),$$

and

$$B(\theta) = \frac{1}{2ik}\sum_l e^{2i\sigma_l}\left[S_l^{l+1/2} - S_l^{l-1/2}\right]P_l^1(\cos\theta).$$

The amplitude A corresponds to scattering in which the spin projection remains constant. The amplitude B describes scattering in which the spin projection flips.

A: 

B: 

Angular distributions -- spin

The differential elastic cross section for an unpolarized incident beam is obtained by averaging the squared magnitudes of the scattering amplitudes over the initial values of the projectile spin and summing over the final ones,

$$\frac{d\sigma}{d\Omega} = \frac{1}{2s+1}\sum_{\nu\nu'}\left|f_{\nu'\nu}(\theta)\right|^2 .$$

For spin-1/2 particles, this becomes

$$\frac{d\sigma}{d\Omega} = \left|A(\theta)\right|^2 + \left|B(\theta)\right|^2 \qquad s = 1/2.$$

For particles of spin ½ and greater, vector and possibly tensor spin observables may be defined in terms of other combinations of the amplitudes. For particles of spin ½, the vector polarization $P(\theta)$ and the spin rotation function $Q(\theta)$ are defined as

$$P(\theta) = \frac{2\,\mathrm{Im}\,A^*(\theta)B(\theta)}{d\sigma/d\Omega} \qquad \text{and} \qquad Q(\theta) = \frac{2\,\mathrm{Re}\,A^*(\theta)B(\theta)}{d\sigma/d\Omega}.$$

Polarization in neutron scattering

The spin-summed angular distribution due to scattering of a polarized beam may be written as

$$\frac{d\sigma_{pol}}{d\Omega} = \frac{d\sigma}{d\Omega}\left(1 + P(\theta)\,\hat{n}\cdot\vec{P}_{pol}\right),$$

where $\vec{P}_{pol}$ is a vector defining the intitial polarization and $\hat{n}$ is the normal to the scattering plane.

The spin-orbit interaction is fairly strong. Its effects on the polarization become visible as soon as partial waves above the s-wave contribute to the scattering.

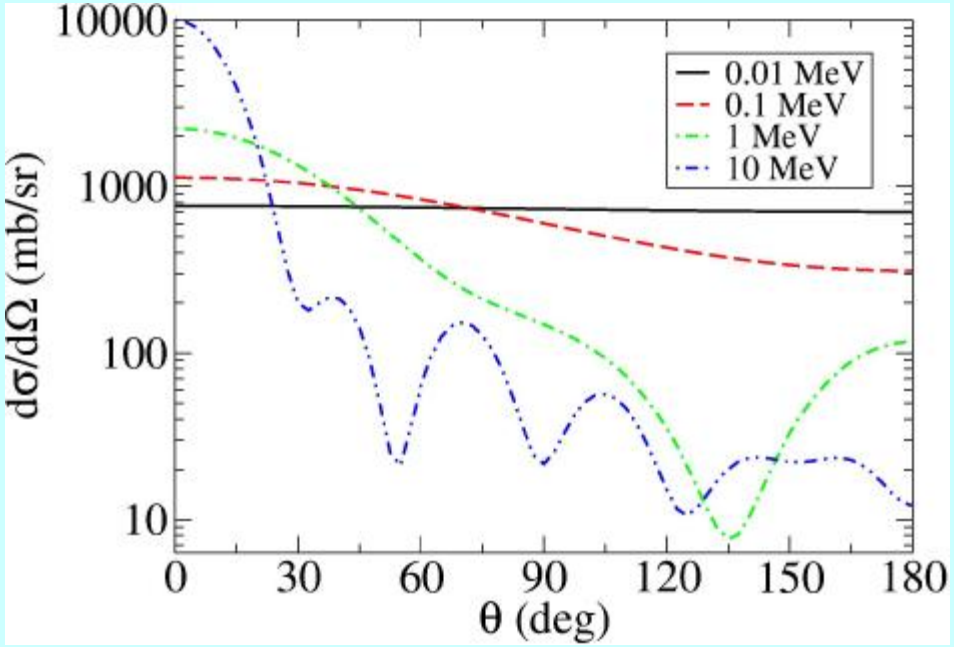

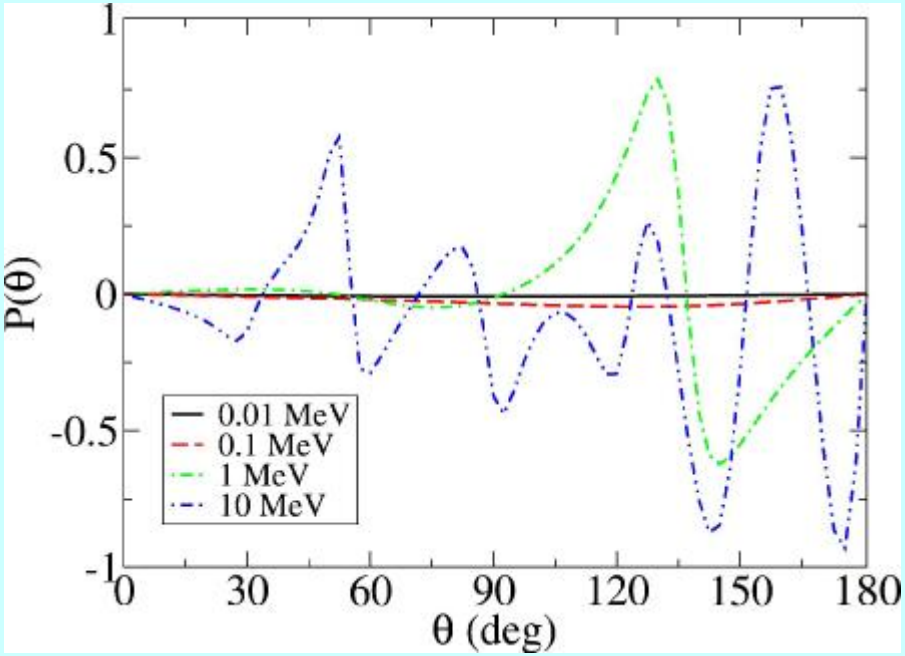

Integrated cross sections -- spin

As before, the absorption cross section may be related to flux lost from the asymptotic probability current density,

$$\sigma_{abs} = -\frac{1}{v}\oint_S \vec{j}\cdot d\vec{S} = \frac{1}{2s+1}\frac{\pi}{k^2}\sum_{lj}(2j+1)\left(1-\left|S_l^j\right|^2\right).$$

The fraction of the flux lost from each partial wave may also be expressed as a transmission coefficient,

$$T_l^j = 1-\left|S_l^j\right|^2.$$

For charged particles, the Coulomb interaction leads to an infinite elastic cross section. For neutrons, integration of the differential cross section yields

$$\sigma_{el} = \int d\Omega \frac{d\sigma}{d\Omega} = \frac{\pi}{2k^2}\sum_{lj}(2j+1)\left|S_l^j - 1\right|^2.$$

For neutron, the total cross section may be defined as the sum of the elastic and absorption ones,

$$\sigma_{tot} = \sigma_{el} + \sigma_{abs} = \frac{\pi}{k^2}\sum_{lj}^{\infty}(2j+1)\left(1-\mathrm{Re}\,S_l^j\right).$$

Comparison with experiment

We recall that, being linear in the scattering amplitude, the total optical cross section may be compare to the energy-averaged experimental one. We see that reasonable agreement with the data is possible here.

We also verified that the partial wave contributions to the energy-averaged elastic cross section,

$$\sigma^{j}_{l,el} = \frac{\pi}{k^2}\left|S^{j}_{l} - 1\right|^2 + \frac{\pi}{k^2}\left\langle \left|S^{j}_{l,fluc}\right|^2 \right\rangle$$

exceed the shape elastic (optical) ones due to contributions from fluctuations. We observe that the fluctuation contributions are negligible only at higher energies.

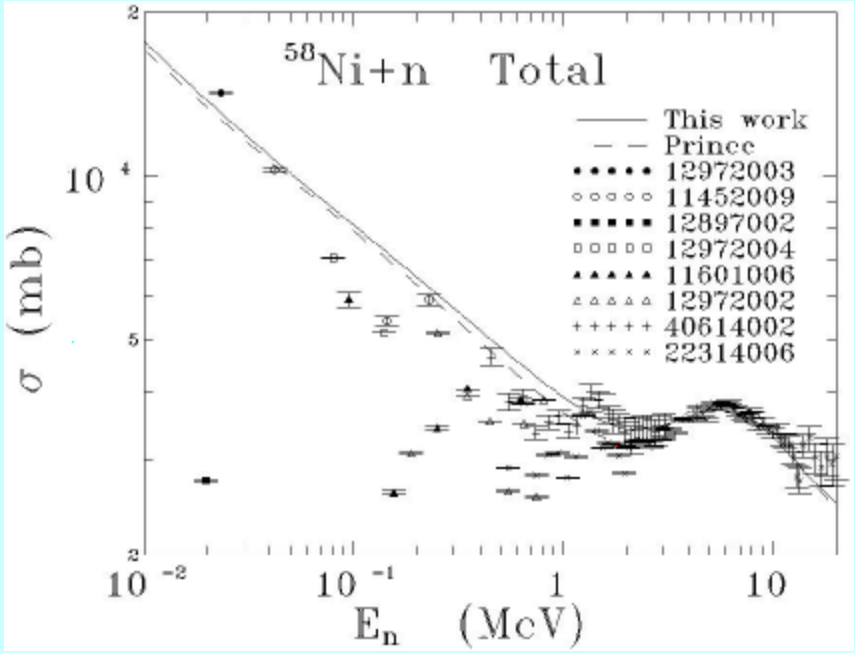

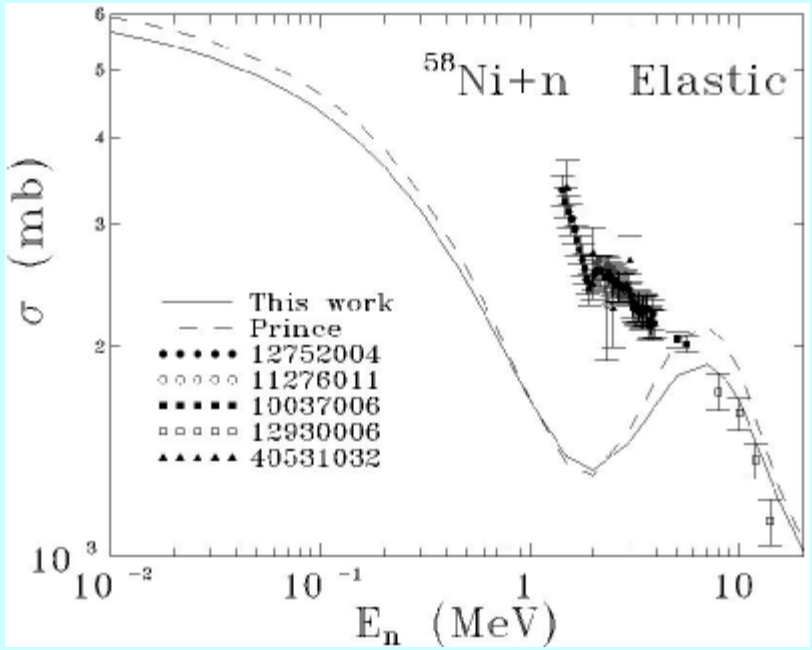

Summary

The objective of the optical model is to describe the fast, direct contribution to nuclear scattering. It makes use of an optical potential with both real and negative imaginary parts. The absorption of flux from the optical wave function, due to the imaginary part of the potential, accounts for the flux lost to the slower, compound nucleus component of the scattering.

The single-channel optical model describes the scattering in the elastic channel alone. It is often called the spherical optical model because, in it, the target may be considered to be spherically symmetric, since its structure is never introduced.

Direct reactions that transfer energy as well as momentum are often quite important. Such inelastic scatterings, in the case of the inert projectiles that we are considering (n, p, α, d, etc.), leave the target in an excited state and diminish the asymptotic kinetic energy of the projectile. To describe inelastic scattering, one must introduce at least the basic characteristics of the ground and excites states of the target. These reactions will be the subject of the next lecture.